ABSTRACT

NUMERICAL STUDIES OF DEEP BED FILTRATION

by
Chan-Gyun Shin

Deep bed filtration is a process used to separate small solid particles suspended in a fluid by using granular solids as the collecting medium. The filter efficiency depends on many parameters such as the Reynolds number, particle drag coefficient, the ratio of the diameter of injected, and filter particles, etc.

In the present work we model the porous media flow (solution of the Navier-Stokes equations) by using a computer code developed by Dr. P. Singh and we restrict our analysis to the case of two dimensional periodic porous media. The computational domain is discretized using the finite element method. In our simulation, the fluid is passing through the periodic porous medium.

One of our objectives is to estimate the range of the drag force that can effect filter efficiency. We study in detail, a range of drag coefficients depending on the Reynolds number, the filter efficiency depending on the size of particle injected, and the number of particles. Last, we study the evolution of the distribution of trapped particles in the filter.

In our model, we find that the filter efficiency is not changed until the drag coefficient, C_D is 10. But in the range of drag coefficient from 10 to 100, the filter efficiency is changed. We find that the filter efficiency is not effected by the number of particles injected and the time step, Δt in the range of $0.0001 - 0.1$. We found that about 40 % of the particles were trapped in top part of the filter. And we can find very similar results when the Reynolds number is 1, 16.556, or 100. The particle distribution results are in qualitative agreement with the available experimental data by Ghidaglia, Arcangelis, Hinch, and Guazzelli [1].

NUMERICAL STUDIES OF DEEP BED FILTRATION

by
Chan-Gyun Shin

A Master's Thesis
Submitted to the Faculty of
New Jersey Institute of Technology
In Partial Fulfillment of the Requirements for the Degree of
Master of Science in Chemical Engineering

Department of Chemical Engineering

May 2000

APPROVAL PAGE

NUMERICAL STUDIES OF DEEP BED FILTRATION

by
Chan-Gyun Shin

Dr. Robert Pfeffer, Thesis Advisor — Date
Distinguished Professor of Chemical Engineering, NJIT

Dr. Pushpendra Singh, Thesis Advisor — Date
Assistant Professor of Mechanical Engineering, NJIT

Dr. Rajesh. N. Dave, Committee Member — Date
Professor of Mechanical Engineering, NJIT

BIOGRAPHICAL SKETCH

Author: Chan-Gyun Shin

Degree: Master of Science in Chemical Engineering

Date: May 2000

Undergraduate and Graduate Education

- Master of Science in Chemical Engineering,
  New Jersey Institute of Technology, Newark, NJ, 2000

- Bachelor of Science in Chemical Engineering,
  Soong-Sil University, Seoul, Korea, 1998

Major: Chemical Engineering

This dissertation is dedicated to my parents

ACKNOWLEDGMENT

The author wishes to express his sincere gratitude to his advisors, Dr. Robert Pfeffer and Dr. Pushpendra Singh, for their guidance, encouragement, and friendship throughout this work.

Special thanks to Dr. Rajesh.N.Dave for serving as a member of the Thesis committee and for all his helpful suggestions.

The author is also grateful to Felix J Alcocer, the senior student who helped me during my research work.

TABLE OF CONTENTS

TABLE OF CONTENTS
(Continued)

Chapter **Page**

LIST OF TABLES

Table **Page**

LIST OF FIGURES

Figures **Page**

LIST OF SYMBOLS

Symbol	
a	*middle of bed width*
B	*single deposited particle of radius*
C_D	*drag force of drag coefficient*
c_{in}	*the number of particles injected into the filter*
c_{eff}	*the number of particles effluent*
d	*diameter of injected particle*
D	*diameter of filter granule*
$d_{p_1p_2}$	*distance between filter granule and injected particle*
E	*The filter efficiency*
e_i	*The efficiency of the ith UBE*
i	*particle number in our model*
j	*released particle position in the filter*
k	*released particle position in the filter*
m	*particle mass*
n	*the number of particles*
p	*particle coordinates*
R_{tube}	*radii of the tubes*
R	*the radius of the filter granule*
r	*the radius of injected particle*
$U_{(0)}$	*fluid velocity given by equation (1.3)*

LIST OF SYMBOLS
(Continued)

Symbol	
u	*fluid velocity*
u_f	*fluid velocity*
u_p	*particle velocity*
W	*Weight*
X	*plane of network*
x	*bed width direction*
x_p	*the particle x-position*
y	*bed width direction*
y_p	*the particle y-position*
α^{-1}	*characteristic pore radius*
ε	*porosity*
ε_{UBE}	*porosity of UBE*
γ	*the position coordinates*
θ	*the position coordinates*
ϕ	*the position coordinates*
φ	*combination corresponds to a value of the ratio between injected particles and filter granule*
ρ_f	*fluid density*
ν	*kinematic viscosity*
Δt	*time step*
ΔZ	*vertical coordinates*

LIST OF SYMBOLS
(Continued)

Symbol	
ΔX	*horizontal coordinates*
$\rho g_{y,}$	*the gravitational force per unit volume in the y direction*
circtr(1,ncir)	*x position in the filter domain*
circtr(2,ncir)	*y position in the filter domain*
delta	*increased value of height to y direction*
Re	*Reynolds number*
λ	*The penetration depth*
ξ	*the characteristic length*
η	*filter efficiency*

CHAPTER 1

INTRODUCTION

1.1 Granular Bed Filtration

1.1.1 Filtration Mechanisums

Filtration is both a process of major contemporary importance and one with its beginning rooted in antiquity. These days, large-scale filters are employed in diverse processes annually treating millions of tons of minerals, chemicals, and liquid wastes. We can easily find common applications of filters for example in automobiles, and exceedingly fine filters are used to ensure the reliable performance of sophisticated navigational and space oriented equipment.

Today, filters are available that function in cryogenic to very elevated temperatures, that remove micrometer size particles in plant-scale operations, that separate low-molecular-weight materials from liquids containing polymeric and other high-molecular-weight species, and that can withstand corrosive fluids.

1.1.2 Deep Bed Filtration vs. Cake Filtration

Filtration can be defined as the process of separating dispersed particles from a dispersing fluid through a porous media. We can consider two kinds of filtration. One is deep bed filtration. The other is cake filtration.

Deep bed filtration is a process used to separate suspended solid particles in a fluid by using a granular media for collecting the particles. If the medium is considered as a multitude of tortuous channels, then for filtration to occur, the particles present must

impact on the walls of the channel and then be retained there by some force. For the particles to impact on the channel walls they must leave the fluid streamlines, and the rate at which this is achieved will depend on the balance of inertial and drag forces experienced by the particles. The medium may be either a bed of granular material or a porous solid. As particles become deposited in the deep bed filter the retentivity becomes greatest at the upstream side of the medium, leading eventually to blockage at these points. Today, deep bed filters are constructed with a graded porosity through the medium, the pores being finest at the downstream side. With particulate media this may be done by using different particle size ranges of material. Deep bed filtration is suitable for the removal of small quantities of solid.

In cake filtration the solid material accumulates on the surface of the medium, so that, after a short initial period, filtration occurs through the bed of deposited solid. This process will continue until the pressure drop across the cake exceeds the maximum permitted by economic or technical considerations, or until all the available void space is filled with solid particles. This method of filtration is the most widely employed in the chemical process industries and is very well suited to the filtration of concentrated suspensions and the recovery of large quantities of solids.

The most important factor in cake filtration is that the permeability or resistance of the filter cake may be controlled, more or less, by altering the particle size distribution of the material, sometimes by adding another solid to it, and also by altering the state of aggregation of the solid.

The difference between cake filtration and deep bed filtration is the manner in which they operate. In the former case, the medium through which the treated suspension flows is composed of the solids to be recovered. The resistance to suspension flow increases with time as a direct result of the increase in filter-cake thickness. For deep bed filtration, deposition occurs throughout the entire medium and the pressure drop increases slowly as the medium becomes increasingly.

The differences between cake and deep bed filtration and the mechanisms they use to separate solids from a fluid do not imply that the two processes embody totally separate and distinct physical phenomena. Because particles present in slurry to be treated by cake filtration invariably cover a wide size range, the finer particles are to a large extent removed by mechanisms like those operating in deep bed filtration. Similarly, even though the deep bed filtration assumes that particle collection takes place throughout the entire filter medium, the extent of deposition within a deep bed filter cannot be made uniform.

Deep bed filtration is a well-established process used to separate solid particles suspended in a fluid. A dilute suspension of particles in a fluid (gas or liquid) is passed through a filter made of porous material. Particles, while flowing through the filter, are trapped inside by various mechanisms. The quantities of main interest are the filter efficiency (the fraction of injected particles trapped in the filter) and the fluid flow. During the filtration process, the transportation and capture of the solid particles in the filtering medium are due to several forces and interactions. The relative importance of these forces is determined by the size of the particle. Deep bed filtration is most

effective and economical in treating large quantities of liquids or gases containing relatively low solid volume fractions of particles of very fine or colloidal size.

A most notable application of deep bed filtration is the use of sand filters for the treatment of water and wastewater. Sand filters in water treatment is well established [11,12] and several recent guidelines have been published dealing with their design [13,14]. Modeling of the slow sand filtration process is essential for a better understanding of the complex behavior of the process and a satisfactory model would be of much help in the operational control of these filter beds. A considerable amount of work on the modeling of deep bed filtration has been achieved to date but interest in the modeling of slow sand filtration has been minimal. Recently Woodward and Ta [15] attempted to simulate slow sand filter performance via a simple, empirical headloss model. Their model was used to forecast flows and headlosses through a network of hydraulically linked slow sand filters, each at a different point in its operating cycle. Deep bed filtration is inherently an unsteady-state process because the motion and deposition of the small particles continuously modify the pore space and thereby the flow pattern is continuously changing. In most of the experimental studies, the process evolution has been followed by measuring the pressure drop between the entrance and the end of the filter (or the permeability of the filter) and the efficiency of the filter (the ratio between the influent and effluent particle concentration). Visualization experiments have also provided information regarding particle deposition and the influence of the filter structure on the flow pattern.

Another application of deep bed filtration is gas cleaning. There are three basic kinds of industrial gas filters: a fabric filter usually in the form of a bag or sleeve, a panel filter usually involving a packed fibrous or granular bed and an aggregate packed or fluidized bed column. Assessment of the performance of filters involves specification of the pressure loss, collection efficiency, and service life factors for both the filter media and the other components of the system. These filters are remarkably reliable. Their useful life seems to be limited only by the filter's material integrity. A granular filter device that incorporates a simple and rather ingenious regeneration technique is the GSC panel-bed filter, developed by Squires and Pfeffer [4].

1.2 Literature Survey and Motivation

The theory of filtration has been studied extensively in the last few decades. As a result, It is possible to simulate the behavior of filter beds under various conditions. For example, recently Ghidaglia, Arcangelis, Hinch, and Guazzelli [1] have attempted to simulate the deep bed filtration of non-Brownian particles carried inside a model porous medium under laminar flow conditions. The porous medium consisted of a random packing of monosize glass spheres of equal size and density. Two batches of glass beads were used with diameters D_1=4.0±0.1 mm and D_2=5.0±0.1 mm. The transparency of glass and the refractive index matched fluid used for the suspension allow direct visual observation inside the whole filter. The movements of particles could be followed in great detail. Such a setup can be used to gain valuable information inside the filter, such as the interaction of particles with the porous medium, and the distribution of trapped

particles. Their filter consisted of a fixed random packing of sphere of equal size a density. The particles to be filled used were coated with a uniformly smooth thin layer of gold using a metal deposition device so they could be clearly tracked in the filter. The first batch had a diameter of 650±40 μm and the second a diameter of 830±30 μm. Two combinations of particles and glass spheres were chosen to study the particle capture inside the random packing.

The carrier fluid was an organic mixture of 60% dibutyl phthalate and 40% butyl benzyl phthalate with a density ρ_f=1.07g/cm3, a kinematic viscosity ν=29 cS and a refractive index of 1.520 at 25 °C. The fluid was Newtonian. The fluid was usually circulated upward through the cell. At the entrance of the cell, the flow was made laminar by using Reynolds numbers based on the length scale of the particles or that of the glass spheres were then always kept at a value smaller than unity. In the first set of experiments, the particles were injected one by one. Each particle was injected as soon as the preceding particle was captured or left the filter and therefore each particle propagated alone in the filter.

The penetration depth was defined as the difference between the initial and final vertical coordinates and the lateral dispersion as the difference between the initial and final horizontal coordinates. From these measurements, the particle penetration depth distribution was determined. They used 200 injected particles so that the experiment would give good statistics. One of their objectives was to analyze the particle capture mechanism when steric effects and hydrodynamic and gravity forces were dominant. In this model, 200 particles were injected one by one in an upward and downward direction.

The distribution was fitted to an exponential decay law and it was also possible to measure the particle lateral dispersion.

It is important to notice that the median value is close to the value of the decay length and to provide a good characterization of the penetration depth of the particles inside the to be perfectly reproducible.

In their study, some aspects of deep bed filtration were visually and statistically studied for small non-Brownian particles flowing into a random packing of monosize glass spheres at low Reynolds number. The particle transport was found to be convective in nature and steric effects and hydrodynamic and gravity forces were found to be dominant.

Pendse, Tien, and Turian [5] studied the hydrodynamic drag force in a uniform flow field acting on a spherical body with small particles attached to its surface. Their objective was to examine the body of available results relating to this flow, to evaluate in detail their efficacy as a practical means for predicting the drag force, to devise effective computational procedures appropriate to each, and to generate experimental data capable of providing critical tests of these results. Their experimental work consists of the measurements of the hydrodynamic drag force acting on spherical particle assemblies similar to those shown in Figure 1-2 when subjected to slowly moving viscous fluid. The method relies on the capability of an electrobalance to detect small changes in the effective weight of the sphere-particle assembly caused by the drag force acting on it. The drag force acting on the assembly, C_D is given by

$$C_D = W_0 - W \tag{1.1}$$

where W_0 is the weight of the test assembly when submerged in a stationary fluid: W is the weight when the assembly is subjected to an upward flow of fluid.In their work, the drag force increase due to the presence of a single deposited particle of radius b is given by:

$$\Delta C_D = 6\pi b\mu U_{(0)} \tag{1.2}$$

where $U_{(0)}$ for a spherical collector is given by the equation

$$\frac{U_{(0)}}{U} = 1 - \left(\frac{a}{r}\right) + \frac{1}{4}\left(\frac{a}{r}\right)\left(1 - \frac{a^2}{r^2}\right)\left(1 - 3\cos^2\theta\right) \tag{1.3}$$

where a is the collector radius b is the particle radius, ΔC_D is the increase in drag force and (γ, θ, ϕ) are the position coordinates of the center of the particle in a spherical coordinate system with the origin at the collector center. Effects of other attached particles on the contribution to the drag force increase due to a given particle can be ignored if the separation distance between the particles is greater than 10 particle radii. Imdakm and Sahimi [3] studied the transport of large particles flowing through porous media. In this paper they develop a novel Monte Carlo method for studying the transport of fine particles in flow through a porous medium and its effect on permeability. They

considered the reduction of the permeability of the porous medium is due to the size-exclusion mechanism and ignored any other factor that can affect the permeability of the pore space. Their porous medium is represented by a two dimensional square network. The bonds of the network, which represent the pore throats of the porous medium, are assumed to be cylindrical capillary tubes which have no converging or diverging section. The radii, R_{tube}, of the tubes are distributed according to a statistical distribution, which, in their paper, is assumed to be a Rayleigh distribution

$$f(R) = 2\alpha^2 R_{tube} \exp(-\alpha^2 R^2) \tag{1.4}$$

where α^{-1} is a characteristic pore radius. This distribution mimics qualitatively the pore-size distributions determined experimentally by several investigators. Creeping flow within each bond is assumed, and the pressure distribution in the network is computed. Their boundary conditions are constant pressures imposed at the entrance and exit plane of the network ($X=0$ and $X=L$, respectively), and matched periodic conditions in the Y direction. They calculate the average flow velocity and flow rate in each bond from the pressure distribution and the bond radii.

Particles are injected into the network at random at plane the $X=0$. They can inject simultaneously a set of M particles into the network at time t=0, the second set at time Δt, and so on, where M can vary from set to set.

Their particles are assumed to be effectively spherical (circular in two dimensions) the effective radii of which are distributed according to a particle-size distribution.

They neglect the possible capture of the particles by the solid surface of the pore.

When a particle arrives at a node, it leaves into one of the attached bonds, which is open to flow. The transition probability for going from one pore into another is assumed to be proportional to the fraction of the flow rate departing from the node through that node. If the particle radius is smaller than the pore radius, the particle is allowed to move into that pore and to be carried with the flow. However if particle radius is big or the same as the pore radius, the entrance to the pore is blocked by the solid particle and the pore is completely plugged. Particle injection is continued until there is no longer any significant change in the network permeability, or until the network is completely plugged and its permeability vanishes. They used networks of size L=40 and 60.

Their results, consist of the variation of the permeability of the network with process time for various Δt, dependence of the permeability of the network on the pore volume injected for various values of Δt, and so on. They were especially interested in the distribution of the distances, along the direction of macroscopic mean velocity that the particles travel before they cause any pore plugging (Figure 1-3). Although the two distributions for the two values of Δt are qualitatively similar, the distance that is traveled by the particles is larger for larger values of Δt. In this figure, we are interested in the distribution of the distance. Lots of particles were trapped in the top of the filter. This result is very similar with our result.

Many studies have been done on the influence of different independent variables on filter performance. Yao et al. were the first to study the particle size effects in filtration [10].

Although from both observations and theory it has been found that the size of suspended particles is one of the most important physical variables influencing deep bed filtration, size is not often measured because the techniques available are time consuming and expensive. Based on their clean-bed filter studies they stated: there exists a critical size at which the suspended particles have minimum removal efficiency. This critical suspended particle size effect is in the order of 1μm (Figure 1-4). Other experimental result shows that the filter efficiency is the lowest for injected particle radius is 3 μm. They also stated that the retention of particles within a filter bed causes changes in the microstructure of the filter medium and as a result of this the behavior of the flow of particles on the filter grains will be significantly affected.

E.Gal, G.Tardos and R. Pfeffer have attempted to calculate filtration efficiency VS Reynolds number [4]. We know that the filtration efficiency is increased when Reynolds number is increased (Figure 1-5).

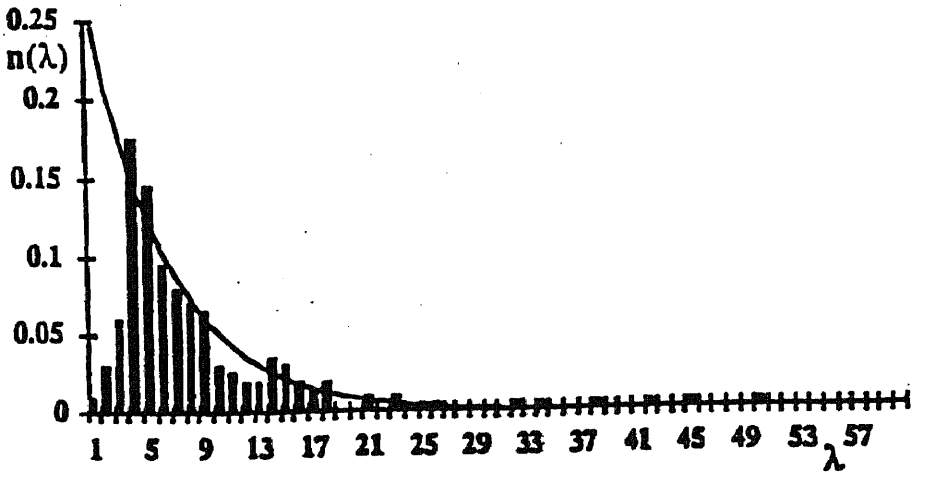

Figure 1-1 Experimental results for the particle penetration depths for $\varphi = 0.162 \pm 0.009$ when particles were injected one by one with an upward flow.

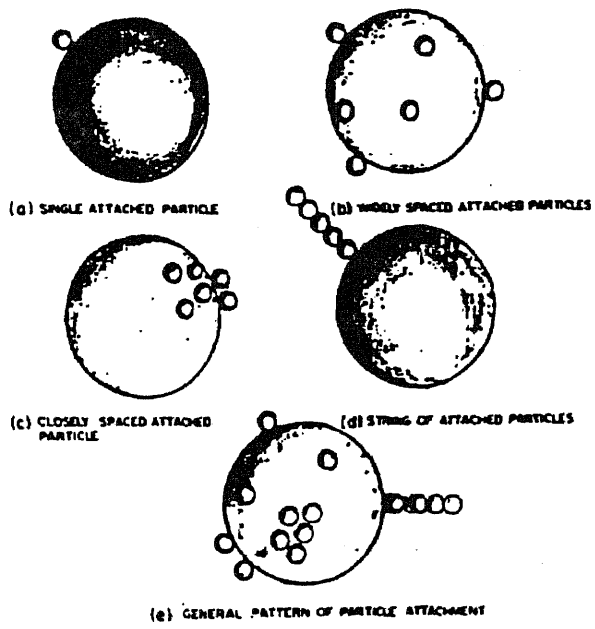

Figure 1-2 Types of collector-particle assemblies

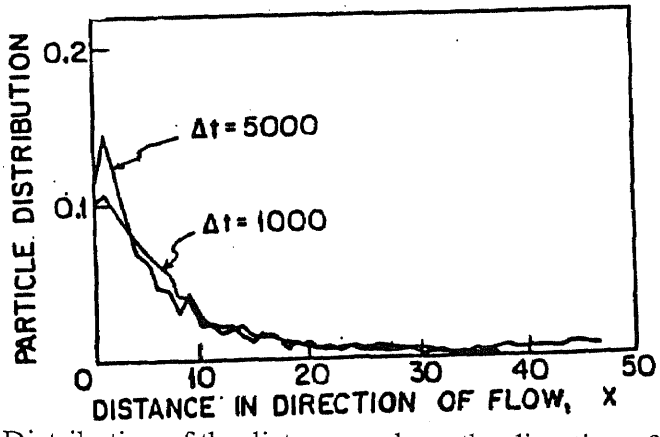

Figure 1-3 Distribution of the distances, along the direction of macroscopic mean velocity that the particles travel before they cause any pore plugging.

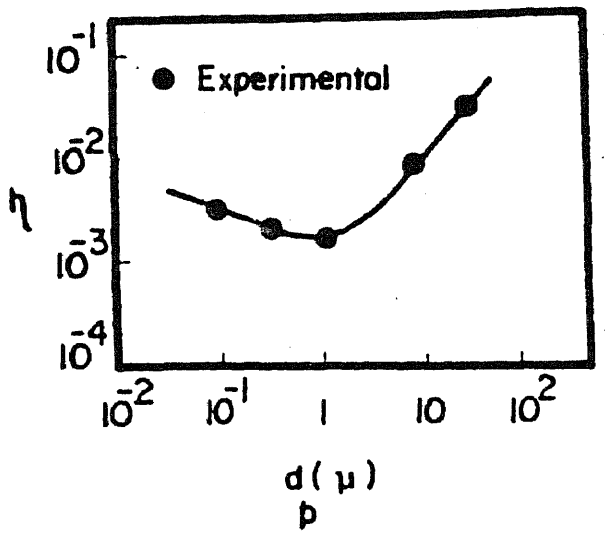

Figure 1-4 This critical suspended particle size effect is in the order of 1μm

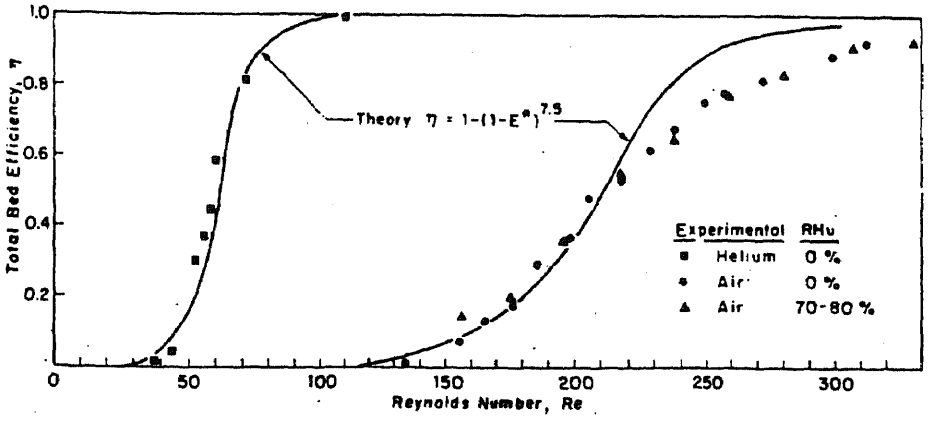

Figure 1-5 Total bed efficiency as a function of Reynolds number for a nine-layer dense cubic bed of spheres. The curves represent trajectory solutions.

CHAPTER 2

MODELING

2.1 Governing Equations

Consider a fluid containing small particles flowing through a filter. The filter consists of two dimensional circular particles of radius R arranged periodically in space as shown in Figure A-1. The flow field in the filter is obtained by solving the Navier-Stokes equations.

$$-\frac{\partial p}{\partial x}+\mu\left(\frac{\partial^2 u}{\partial x^2}+\frac{\partial^2 u}{\partial y^2}\right)=\rho\frac{du}{dt} \tag{2-1}$$

$$\rho g_y-\frac{\partial p}{\partial y}+\mu\left(\frac{\partial^2 v}{\partial x^2}+\frac{\partial^2 v}{\partial y^2}\right)=\rho\frac{dv}{dt} \tag{2-2}$$

where ρg_y is the gravitational forces per unit volume in the y direction.

In the simulation, the fluid is passing through a periodic porous medium in which the solid particles are represented by the circles. The porous medium is periodic, and thus the no-slip boundary conditions apply on the walls and on the particle surfaces. A typical computational domain can be seen in the Figure A-2. The velocity u_f is known at center of the inlet, and for our simulations we are assuming a value of u_f =1.0, the traction boundary conditions are specified at the exit.

$$m\frac{dv_p}{dt}=C_D(u_f-u_p) \tag{2-3}$$

$$m\frac{dv_p}{dt} = f \tag{2-4}$$

$$u_{p_{n+1}} = u_{p_n} + fdt \tag{2-5}$$

where m = *particle mass*

C_D = *drag coefficient*

u_p = *particle velocity*

u_f = *fluid velocity*

In our work we will assume that the velocity field obtained above remains valid when small particles are injected along with the fluid. This assumption is reasonable provided the volume concentration of injected particles sufficiently small. In this limit of small concentration the motion of a small particle in governed by Equation 2-4, where f is the hydrodynamic force acting on the particle. We will further assume that the Reynolds number based on the relative velocity of the fluid and particle is small. There C_D is inversely proportional to the Reynolds number.

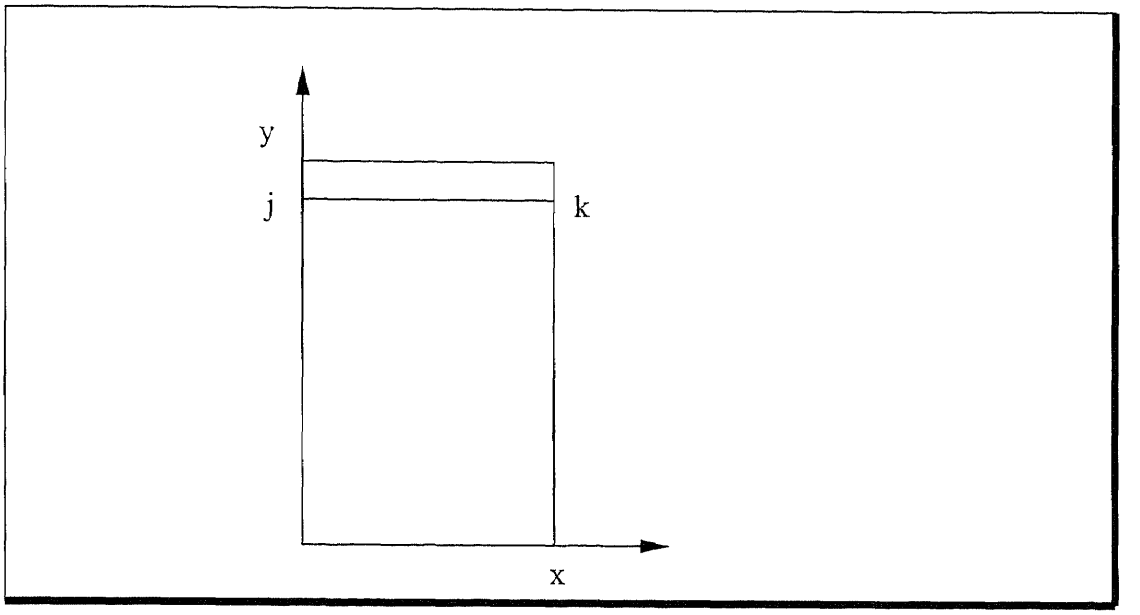

Figure 2-1. The filter domain

In this study, we injecte a single particle at a time into the filter. The initial velocity of the particle is taken to be zero. The particles are released at y=19, (see Figure A-1) and the value of x is varied to sample the channel width. A large number of particles are released at different uniformly distributed values of x (Line j-k in Figure 2-1).

The trajectories of there particles are used to study the behavior of the filter. The number of particles released is increased until the statistical properties of the filter become independent of this number. The time step used in the calculation is decreased to a value such that the results become independent of the time step.

2.1.1 Filter Efficiency

The filter efficiency E, defined as

$$E = \frac{c_{in} - c_{eff}}{c_{in}} \tag{2-6}$$

where c_{in} is the number of particles injected into the filter and c_{eff} is the number of particles that are not trapped inside the filter. Therefore when E=1 all particles are captured inside the filter and when E=0 all particles escape the filter.

2.1.2 Trajectory Calculation

The particle trajectories are calculated by integrating equation (2-4) using the following second order scheme:

$$x_{p_{n+1}} = x_{p_n} + \frac{u_{p_n} + u_{p_{n+1}}}{2}(\Delta t) \tag{2-7}$$

$$y_{p_{n+1}} = y_{p_n} + \frac{u_{p_n} + u_{p_{n+1}}}{2}(\Delta t) \tag{2-8}$$

where x_p , y_p is the particle position and Δt is the time step. These trajectories can be determined when the particle velocity at the present and the previous time steps are known.

When the particles are injected one by one, their trajectories inside the filter are calculated from the equation (2-7,2-8). As particles move toward the filter granule, their trajectories deviate from streamlines, and some of them may intersect with the filter granule.

2.1.3 Particle Capture

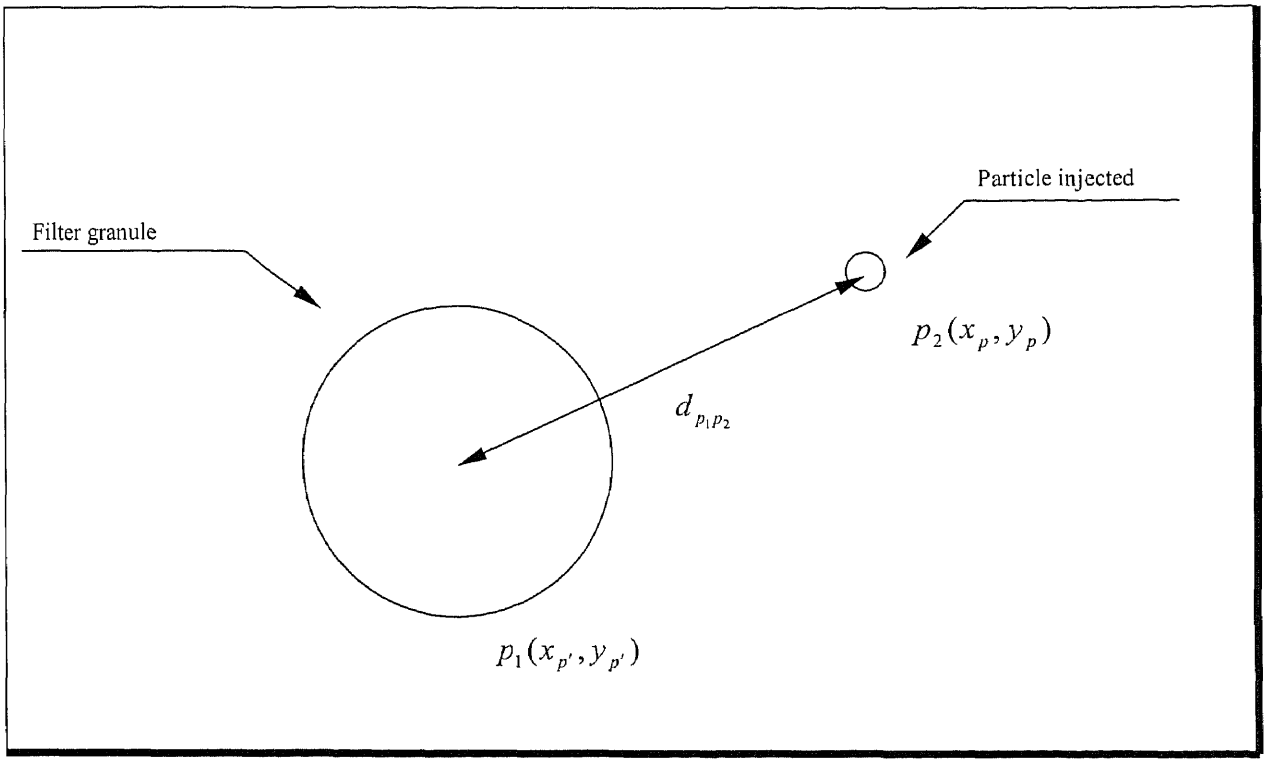

Figure 2-2 Particle capture between granule in the filter and particle injected

Figure 2-2 shows a filter granule and an injected particle moving close to the filter granule. The radius of the filter granule is R and its position is p_1. The radius of the injected particle is r and its position is p_2. We will assume that an injected particle is captured if it touches a filter granule. The distance between the filter granule and injected particle is given by

$$d_{p_1p_2} = \sqrt{(x_{p'} - x_p(t))^2 + (y_{p'} - y_p(t))^2} \tag{2-9}$$

$$d_{p_1p_2} \leq R + r \tag{2-10}$$

where $x_p(t)$ and $y_p(t)$ are the time dependent position of the injected particles. If the trajectory of the injected particle is such that $d_{p_1p_2} \leq R + r$ at some time, i.e., the particles overlap, we will assume that the injected particle is captured at the surface of the filter granule. If a particle moves out of the domain without touching or colliding with any filter particle, we will assume that it is not captured.

2.2 Domain

The filter domain used in our simulations is formed by placing granules on a periodic lattice as shown in Figure A-1. All lengths have been made dimensionless by scaling with the filter granule radius. The radius of the filter granule is assumed to be 0.35, and the distance between them in the flow direction is 1.2 and in the cross stream direction is 0.8. For these parameter values the porosity of the filter is equal to 0.639, where the porosity ε is defined to be

$$\varepsilon = \frac{\text{area coverd by the fluid}}{\text{area of the bed}} = 1 - \frac{\text{area of filter granules}}{\text{area of bed}} \qquad (2\text{-}11)$$

2.2.1 Injected Particle

The injected particles are assumed to have a fixed radius which is varied to study the effect of r on the filter efficiency. In our simulations, the radius of injected particle, r is varied between 0.01 and 0.0001.

2.2.2 Filter Granule

We position the filter granules using equation below,

$$\text{circtr}(1,\text{ncir})=1.0 + (\text{i-1})*1.2 \text{ or } \text{circtr}(1,\text{ncir})=1.60 + (\text{i-1})*1.2 \quad (2\text{-}12)$$

$$\text{circtr}(2,\text{ncir})=2.0+ \text{delta} \quad (2\text{-}13)$$

where circtr(1,ncir) is the x position on the filter domain and circtr(2,ncir) is the y position on the filter domain and i is the number of the particle in our model (i = 9 particles per row) and delta (= 0.8) is the distance between the particles in the direction of flow.

2.2.3 Filter Granule Reynolds Number

The particle Reynolds number is calculated from the equation below,

$$\text{Re} = \frac{u_f D}{\nu} \quad (2\text{-}14)$$

where ν is kinematic viscosity. In our model, filter granule diameter, D is 0.7 and fluid velocity u_f is 1. We want to try to simulate low Reynolds number. To obtain the three particle Reynolds numbers 1, 16.556, and 100, we use a kinematic viscosity ($\nu = 7.0*10^{-1}$ for a Reynolds number =1, $\nu = 4.2*10^{-2}$ for a Reynolds number =16.556, and $\nu = 7.0*10^{-3}$ for a Reynolds number =100).

2.2.4 Boundary Condition

The velocity u_f is assumed at the inlet, and at the exit,

$$u|_{inlet\,/\,exit} = \frac{x(2a-x)}{a^2} \tag{2-15}$$

where 2a is the bed width. The maximum fluid velocity of 1 is at x = a. The no slip velocity boundary condition is applied at the surface of filter particles and the periodic boundary:

$$\begin{cases} u = 0 \\ \dfrac{\partial u}{\partial y} = 0 \end{cases} \tag{2-16}$$

is applied at the side walls of the domain.

One of the objectives of this work was to analyze the particle capture mechanism when hydrodynamic and drag forces were dominant. It is, however, important to estimate the influence of other forces, such as inertial, electrostatic, Brownian, and molecular forces in this process.

2.2.5 Model Representation of The Filter Bed

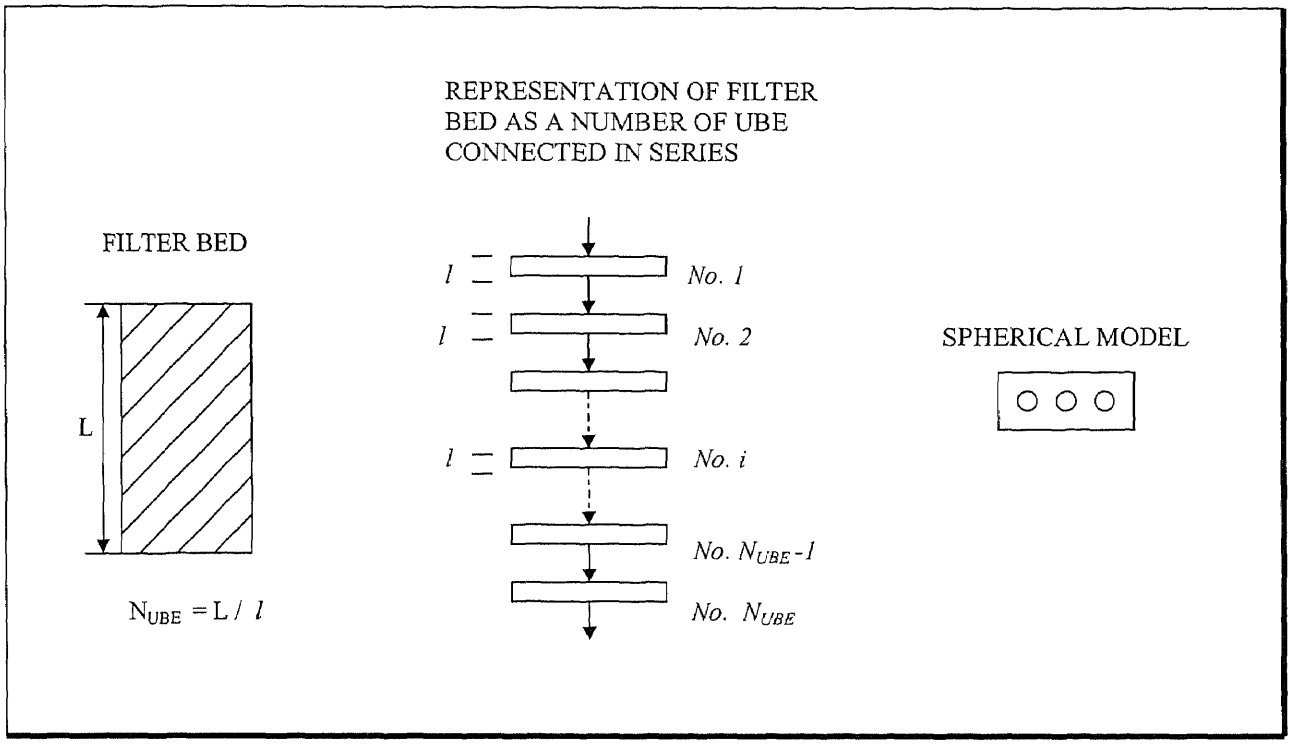

Figure 2-3 Schematic representation of granular media.

The principle involved in the theoretical calculation is as follows. A filter bed can be viewed an as assembly of particle collectors. Using the terminology of Payatakes, Tien, and Turian, [9] a filter bed can be considered as a series of unit bed elements (UBE), each of which, in turn, is composed of a number of collectors. In Figure 2-3 and Figure A-6, we show the filter, and total number of UBE's; N_{UBE} is 20 UBE's. we take the Height of one UBE, *l* is 0.8. And Each UBE has 9 spherical granules.

If a granular filter is viewed as an assembly of collectors, as depicted in Figure 2-3, it is natural to express the filter's intrinsic ability to collect particles in terms of the collection efficiency of each of the unit bed elements. First, recall that a filter performance is

described by its overall efficiency E, defined as Equation 2-6. where c_{in} and c_{eff} denote the influent and effluent particle concentrations, respectively.

The overall collection efficiency can easily be expressed in terms of the unit collector efficiencies (Overall collection efficiency = Σ unit collector efficiency). Referring to Figure 2-3, let c_i denote the particle concentration of the suspension exiting the *i*th UBE. The efficiency of the *i*th UBE (or the *i*th unit collector) e_i (or the *i*th unit collector efficiency) is

$$e_i = \frac{c_i}{c_{in}} \tag{2-15}$$

where N_{UBE} is the total number of UBEs. The total number N_{UBE} of UBEs in series for a filter of height L is

$$N_{\text{UBE}} = \frac{L}{l} \tag{2-16}$$

or more precisely, N_{UBE} should be taken as the integer closest to the value of L/l.

The porosity of the UBE is

$$\varepsilon_{UBE} = \frac{\text{area coverd by the fluid}}{\text{area of the bed}} = 1 - \frac{\text{area of filter granules}}{\text{area of bed}}$$

$$= 1 - \frac{0.35 * 0.35 * \pi * 9}{12 * 0.8} = 0.639 \tag{2-17}$$

CHAPTER 3

NUMERICAL RESULTS

In our simulations the filter bed depth is 20 and the width is 12. If the filter domain is too small, the injected particles will be affected by the side walls velocity of the filter, and the model will not represent the filter properly near the walls. And if the filter domain is large, computational time will be increased. We formed the filter by placing 180 spherical granules of radius 0.35 periodically. The porosity of the filter is 0.639.

The flow inside the filter is obtained by solving Navier-Stokes equations (Equation 2-1, and 2-2) using Dr. P. Singh's code. The in and out flows are assumed to be parabolic and the periodic boundary conditions are applied at the two side walls. The velocity is forced to be zero on the surface of filter granules.

The particles to be trapped are released at the top of the filter bed. The initial velocity of these particles is assumed to be zero. The particles move with the by flowing fluid. Some particles are trapped and some pass through the filter. If a particle collides with the filter particle we assume that it is captured by the filter. The summary of simulation results is in appendix B, C, D

3.1 Convergence of Results

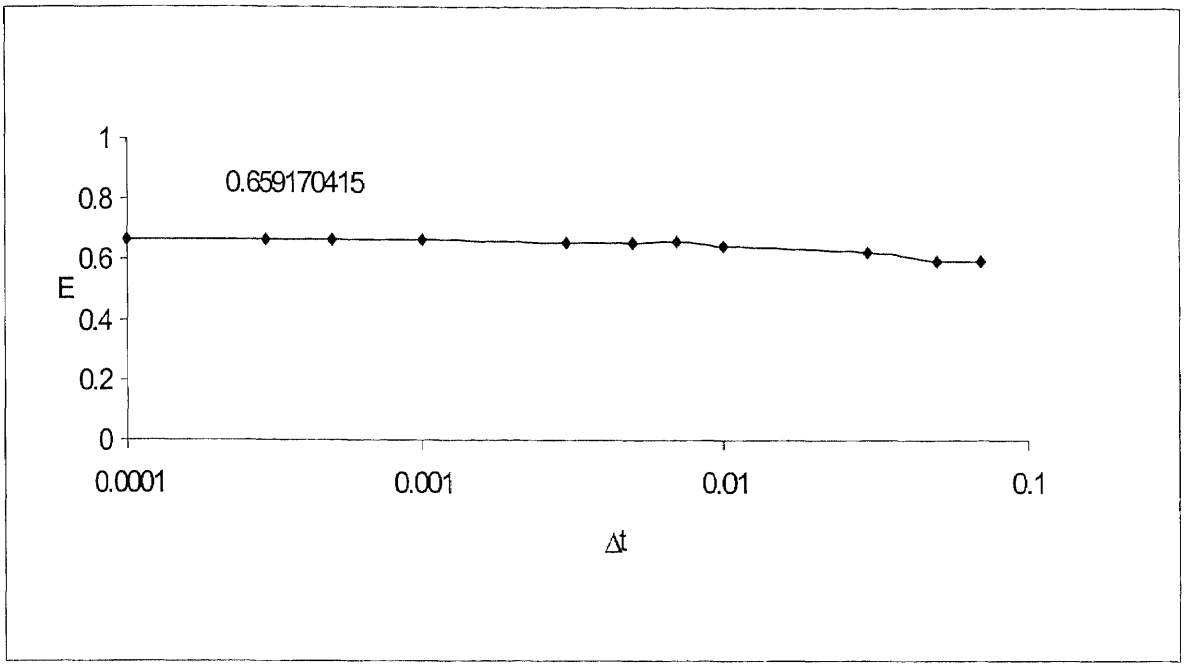

Figure 3-1 Numerical results for the particle efficiency when Δt is changed.

After the fluid velocity flow field is determined by the solving Navier-Stokes equations, the particles are injected into the filter domain at plane y = 20. The drag coefficient is 20. The injected particle radius, r, is 0.001. In order to ensure that the time step used in our simulation is sufficiently small we varied Δt. These results are shown in figure 3-1 which shows that the filter efficiency becomes independent of Δt used.

3.2 Particles Radius

The particles of radius r were injected into the periodic packing of granular filter with radius R. Figure 3-2 shows the efficiency of 500 particles injected one by one. The drag coefficient C_D is 20.

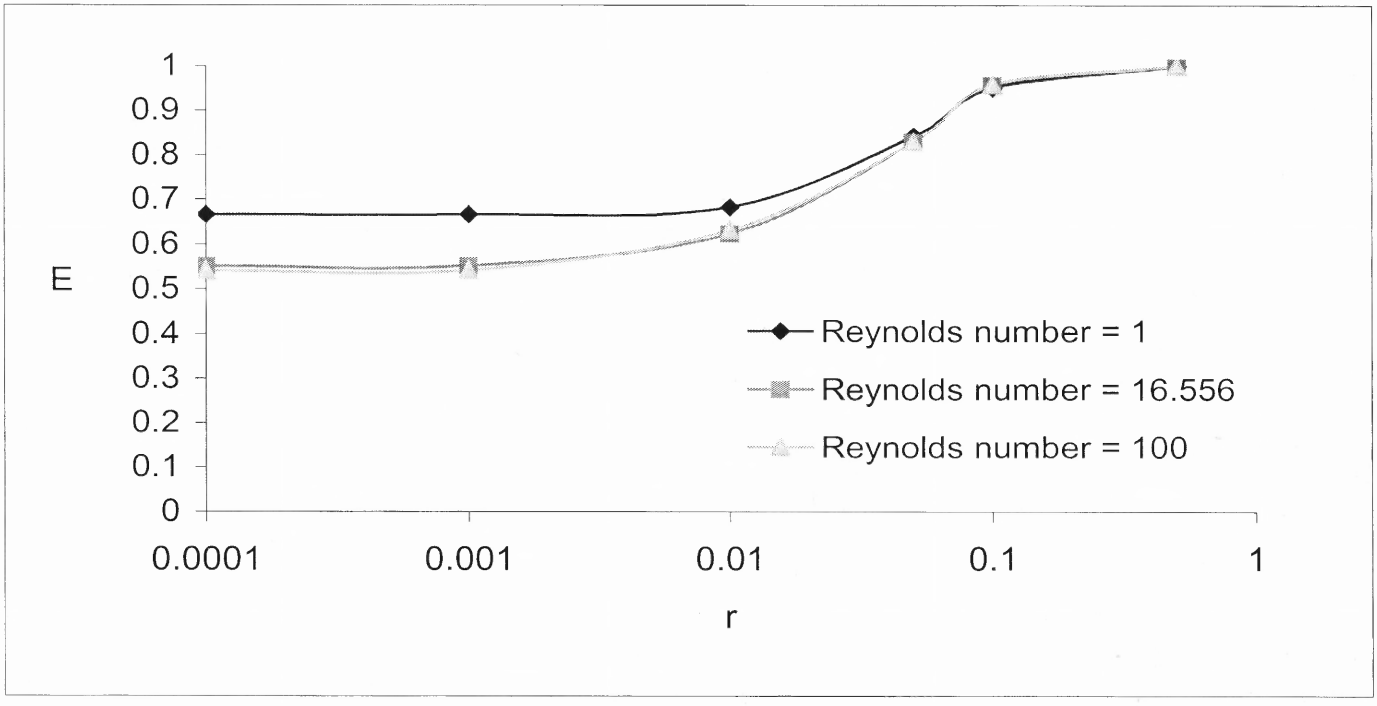

Figure 3-2 Numerical results for the injected particle radius. When radius of particle, r is increased.

When the particle radius is increased, the filter efficiency is also increased. But when r increase from 0.00001 to 0.001, the filter efficiency is not changed. From r = 0.001, filter efficiency increases and when r is above 0.1, the particles injected are all trapped in the filter domain.

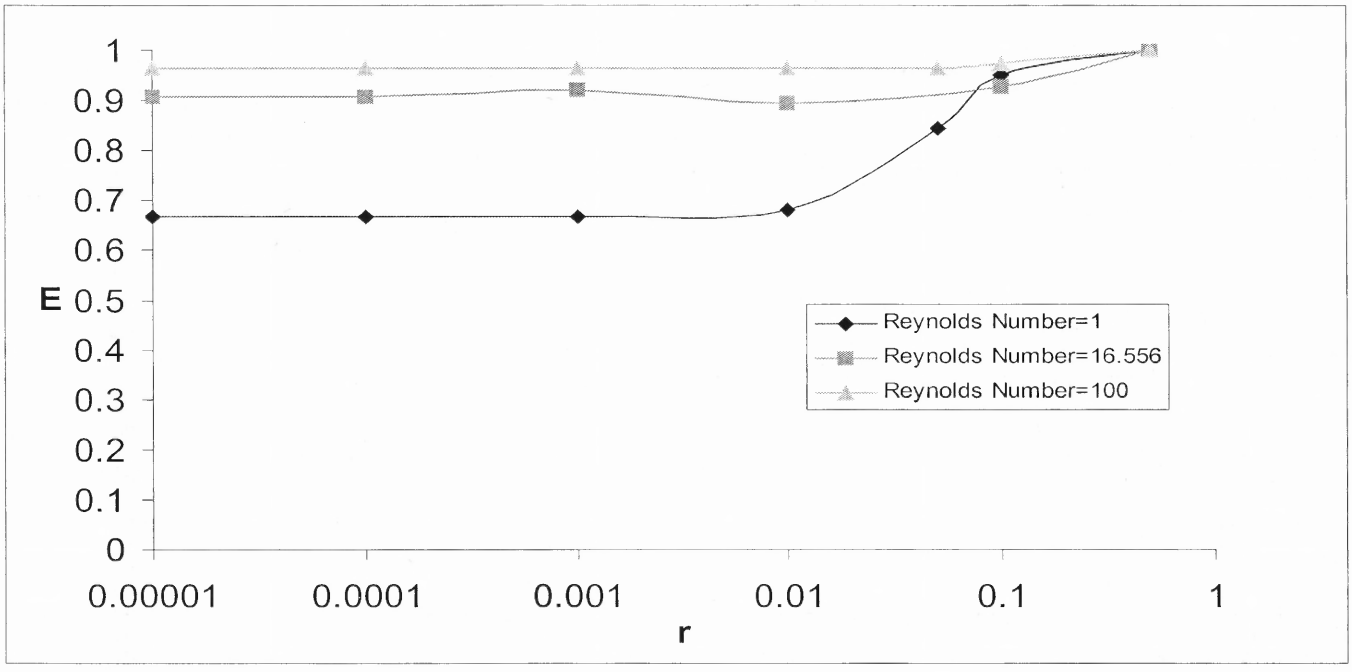

Figure 3-3 Numerical results for the injected particle radius. When radius of particle, r is increased. And we are using a different C_D for different Reynolds number.

Here use a different drag coefficient, C_D because changing the Reynolds number results in a different drag coefficient (C_D =20 for Reynolds number =1, C_D =1.2 for Reynolds number =16.556, C_D =0.2 for Reynolds number =100). The drag coefficient is estimated as equations below

If C_{D_1} and v_1 are the drag coefficient and kinemetic viscosity for Reynolds number = 1, then

$$C_{D_1}\frac{v_{16.556}}{v_1} = C_{D_{16.556}} \qquad \text{for Reynolds number =16.556} \qquad (3\text{-}1)$$

$$C_{D_1}\frac{v_{100}}{v_1} = C_{D_{100}} \qquad \text{for Reynolds number =100} \qquad (3\text{-}2)$$

E.Gal, G.Tardos and R. Pfeffer [4] have attempted to calculate filtration efficiency vs. Reynolds number. We know that the filtration efficiency is increased when the Reynolds number is increased (Figure 1-5).

Yao et al. (1970) were the first to study the particle size effects in filtration [10]. Based on their clean-bed filter studies they stated: there exists a critical size at which the suspended particles have minimum removal efficiency. This critical suspended particle size effect is in the order of $1\mu m$ (Figure 1-4). They also stated that the retention of particles within a filter bed causes changes in the microstructure of the filter medium and as a result of this the behavior of the flow of particles on the filter grains will be significantly affected. Figure 1-4 shows the collector efficiency of particles of different sizes. Our result is in range > 1. We know that the filter efficiency is increasing between 1 and 10^2. Our model has also similar result. (Figure 3-2, 3-3)

3.3 Drag Coefficient

In this section, we show that the role of drag coefficient which is a function of particle Reynolds number on the filtration efficiency.

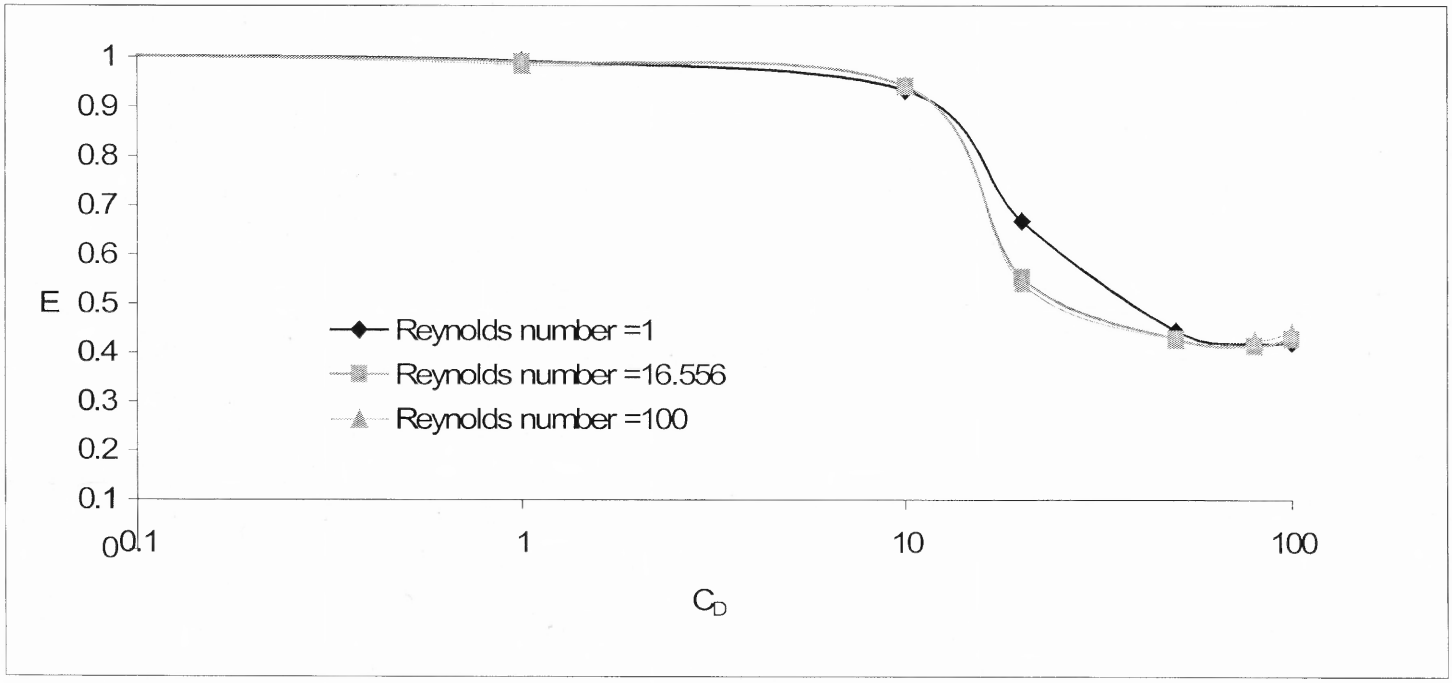

Figure 3-4 Numerical results for the filtration efficiency when the drag coefficient when it is changed

Figure 3-4 shows that the overall efficiency of 500 particles injected one by one in the case of downward flow and for r = 0.001. The figure shows that filter efficiency depends on the drag coefficient, only when C_D is between 10 and 100. For $C_D < 10$, the filter efficiency is approximately one and for $C_D > 100$ the filter efficiency is again constant. This graph shows the filter efficiency is high when Reynolds number is low. Because filter efficiency is depended on many factors, one is filter granule's Reynolds number, the other is injected particle's Reynolds number. We only changed the filter granule's Reynolds number.

3.4 Number of Particles

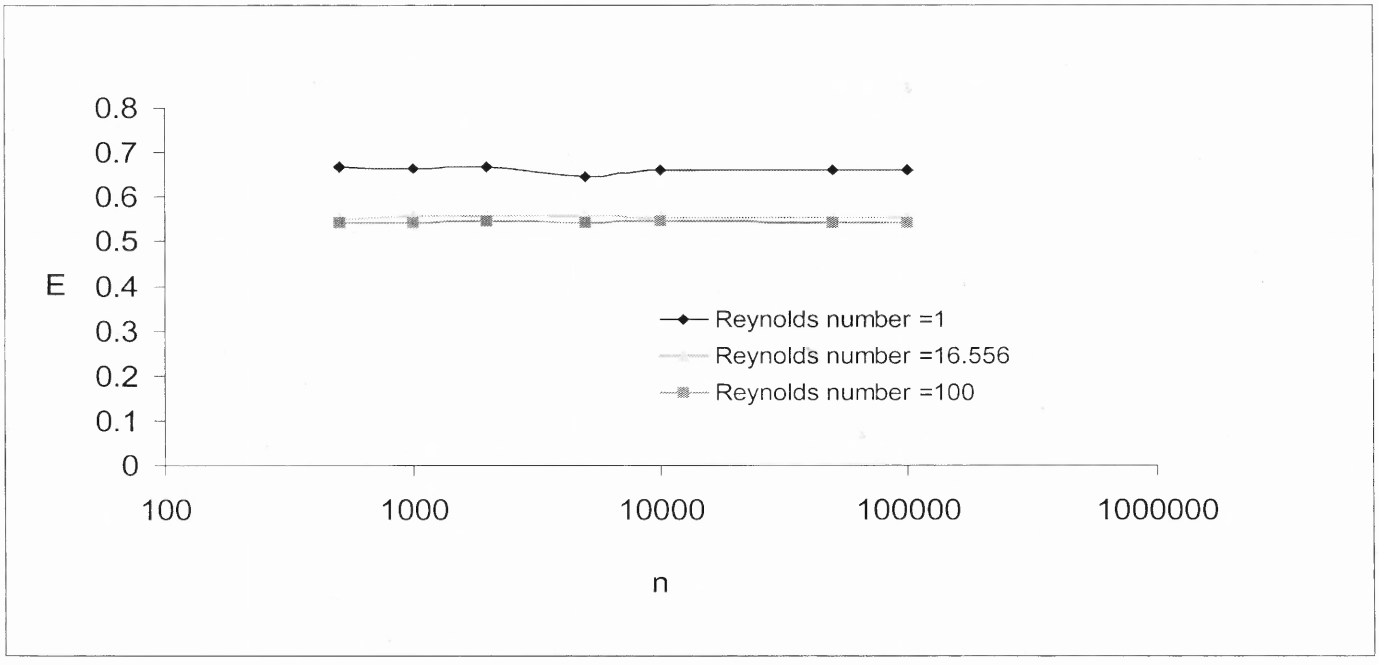

Figure 3-5 Numerical results for particle efficiency when number of particle increases. The drag coefficient (C_D) is 20 and the time step (Δt) is 0.001.

Figure 3-5 shows the dependence of efficiency on the number of particles injected into the domain. We injected 500, 1000, 2000, 5000, 10000, 50000 and 100000 number of

particles at equally spaced positions along the inlet. The injected particle radius, r = 0.001. When the Reynolds number is 1 the filtration efficiency is 0.645~0.666. When the Reynolds number is 16.556 and we injected 500~100000 number of particles, and filtration efficiency is 0.550~0.555. When the Reynolds number is 100, the filtration efficiency is 0.540~0.544. In all three cases the filter efficiency in approximately independent of the number of particles injected into the domain. We fixed drag coefficient C_D= 20 for each Reynolds number.

3.5 Penetration of Depth Distribution

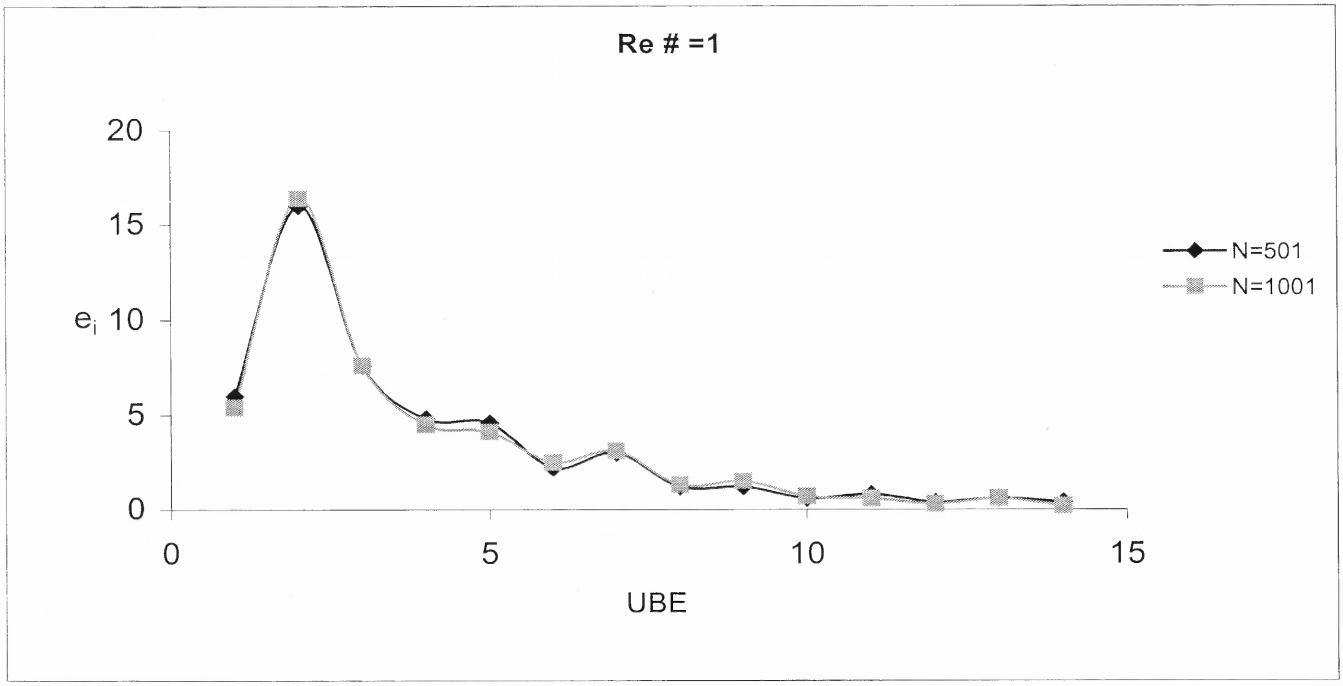

Figure 3-6 Numerical results for the particle penetration depths for Reynolds number=1. where e_i is efficiency of the *i*th UBE in the filter and N is a number of injected particles

Figure 3-6 shows the penetration depth distribution for 500 particles and for 1000 particles injected one by one, for r = 0.001. The drag coefficient, C_D is 20, and the time

step, Δt is 0.001. All lengths have been made dimensionless by scaling with the filter particle radius. The number of injected particles captured at a given depth is denoted by e_i. About 40 % particles were trapped in the top part of the filter. We find that the results for the three Reynolds number 1, 16.556, and 100, are qualitatively similar.

Figure 1-1, obtained experimentally is in excellent agreement with our numerical results. In this model, 200 particles were injected one by one in an upward flow of fluid and for $\varphi = 0.162 \pm 0.009$. The distribution was fitted to an exponential decay law, $\exp(-\lambda/\xi)$ with $\lambda = \Delta Z / D$. The penetration depth was defined as the difference between the initial and final vertical coordinates, ΔZ, and the lateral dispersion as the difference between the initial and final horizontal coordinates, ΔX. From these measurements, the particle penetration depth distribution was determined, in the case of one by one injection, it is also possible to measure the particle lateral dispersion.

It is important to note that the median value is close to the value of the decay length and provides a good characterization of the penetration depth of the particles inside the medium. For a given value of the φ, the experiments were found to be perfectly reproducible.

CHAPTER 4

CONCLUSIONS AND DISCUSSION

In this study, some aspects of deep bed filtration have been numerically studied for small particles flowing into the periodic packing of granular particles at three values of the Reynolds number. We studied deep bed filtration. The porous medium was represented by a two dimensional model of spherical collectors. The primary quantities of interest were the effect of drag coefficient, and Reynolds number, and particle size on the filtration efficiency and particle penetration depth.

The ranges of the drag force were examined for different Reynolds number, i.e., *Re=1*, *Re=16.556* and *Re=100*. It was discovered that drag coefficient range, C_D *=10~100* will change the filter efficiency. We found that the filter efficiency depends on the size of particle injected. We examined different particle size injected into the filter one by one. When r is changed from 0.00001 to 0.001, the filter efficiency is not changed. From injected particle radius, r = 0.001, the filter efficiency increased and when r is above 0.1, the particles injected trapped were all trapped in the filter domain. We also found that the curves of Reynolds numbers 16.556 and Reynolds number 100 were similar.

We found the penetration depth distribution. These distributions were examined for different numbers of particle injected into the filter. About 40% of the injected particles were trapped in the top of the filter. These results are in qualitative agreement with the available experimental data.

Using numerical simulation we successfully reproduced the results of experimental work on deep bed filtration that has spherical filter granules for various Reynolds number

based on filter granule. Thus we can use this code for different parameter values to suit a desired application. This would be far less cumbersome then to setting up experiments for different parameters.

APPENDIX A

FILTER DOMAIN

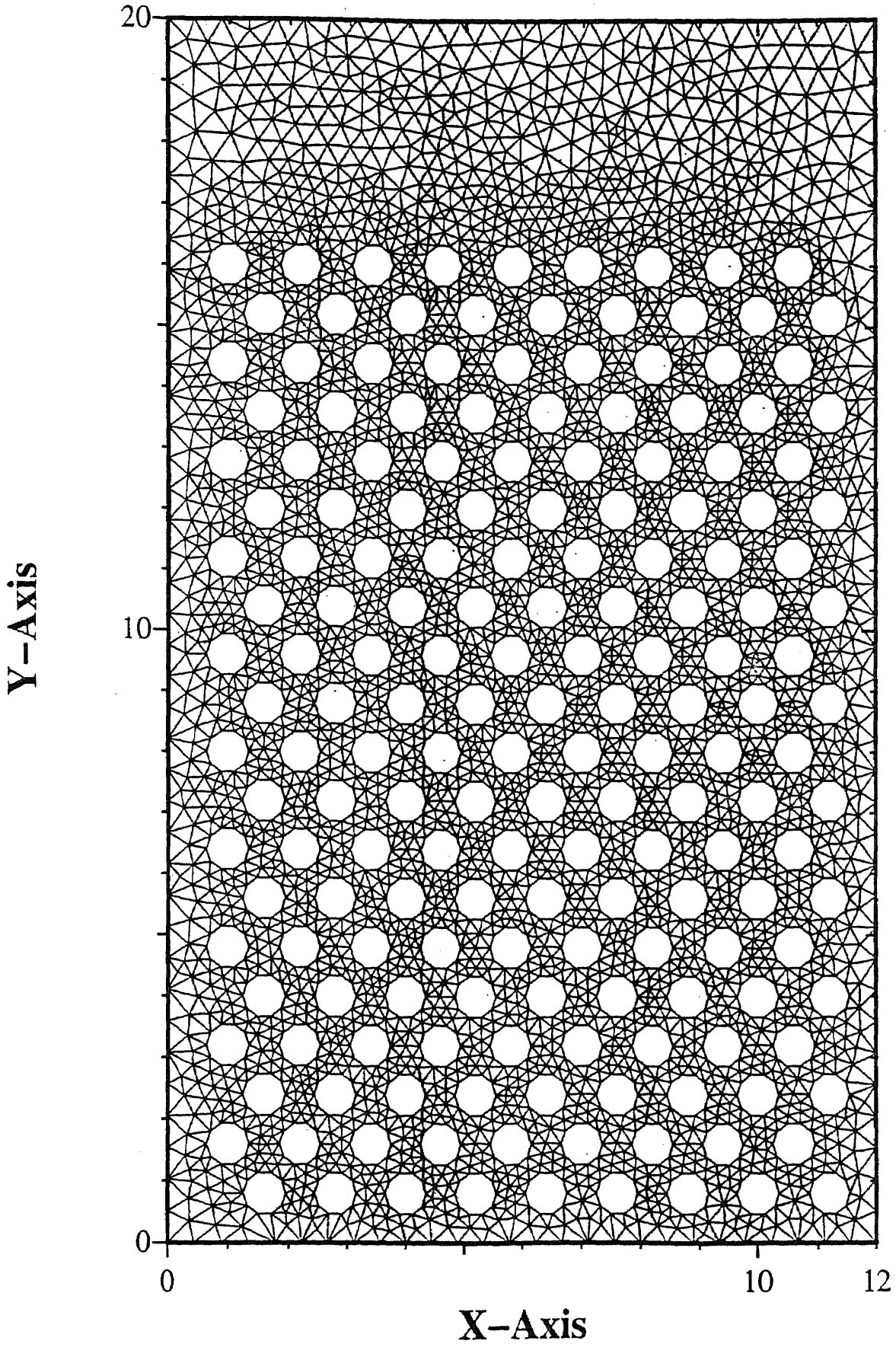

Figure A-1 Filter mesh by using finite element method

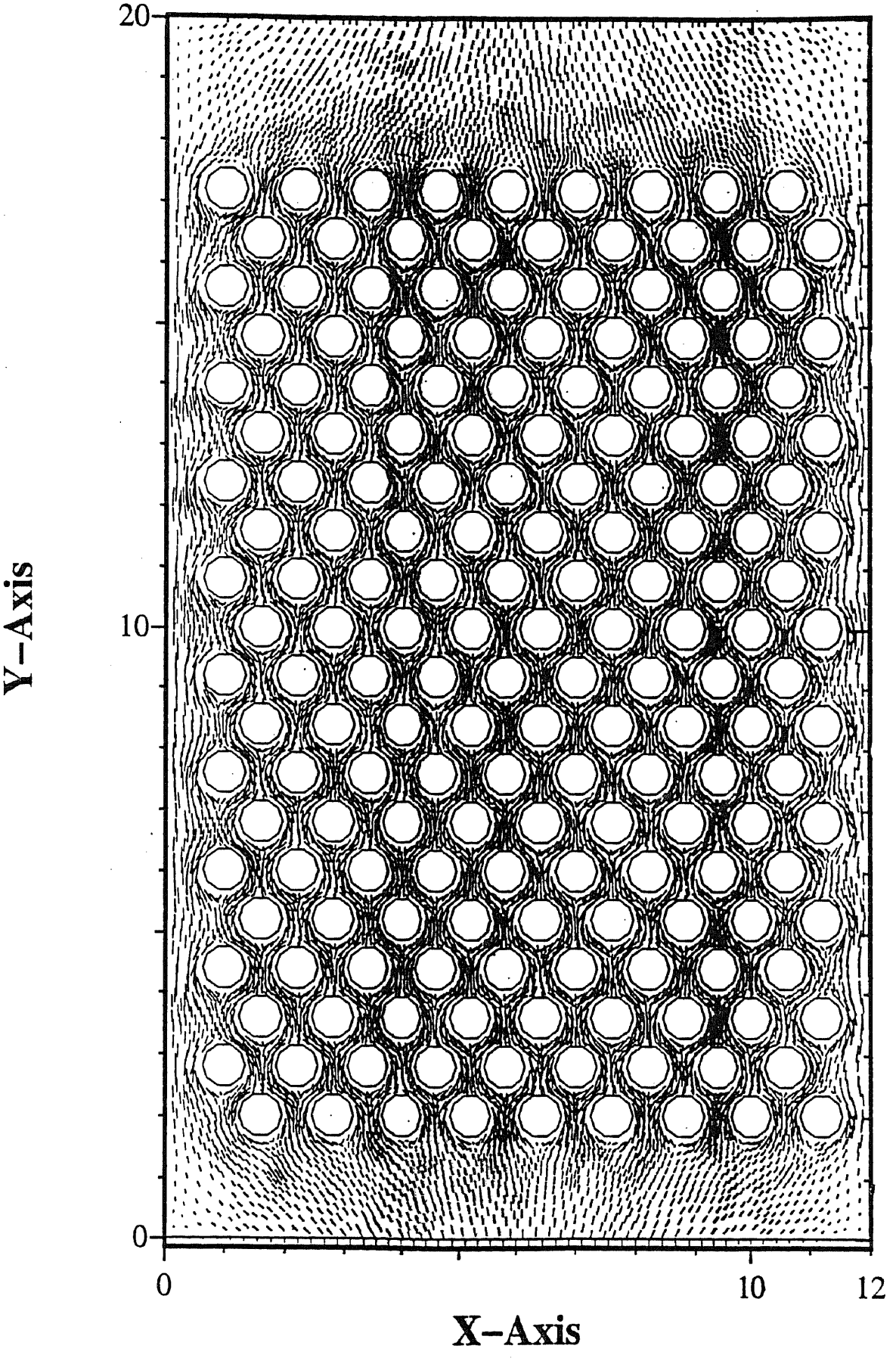

Figure A-2 Filter velocity profile

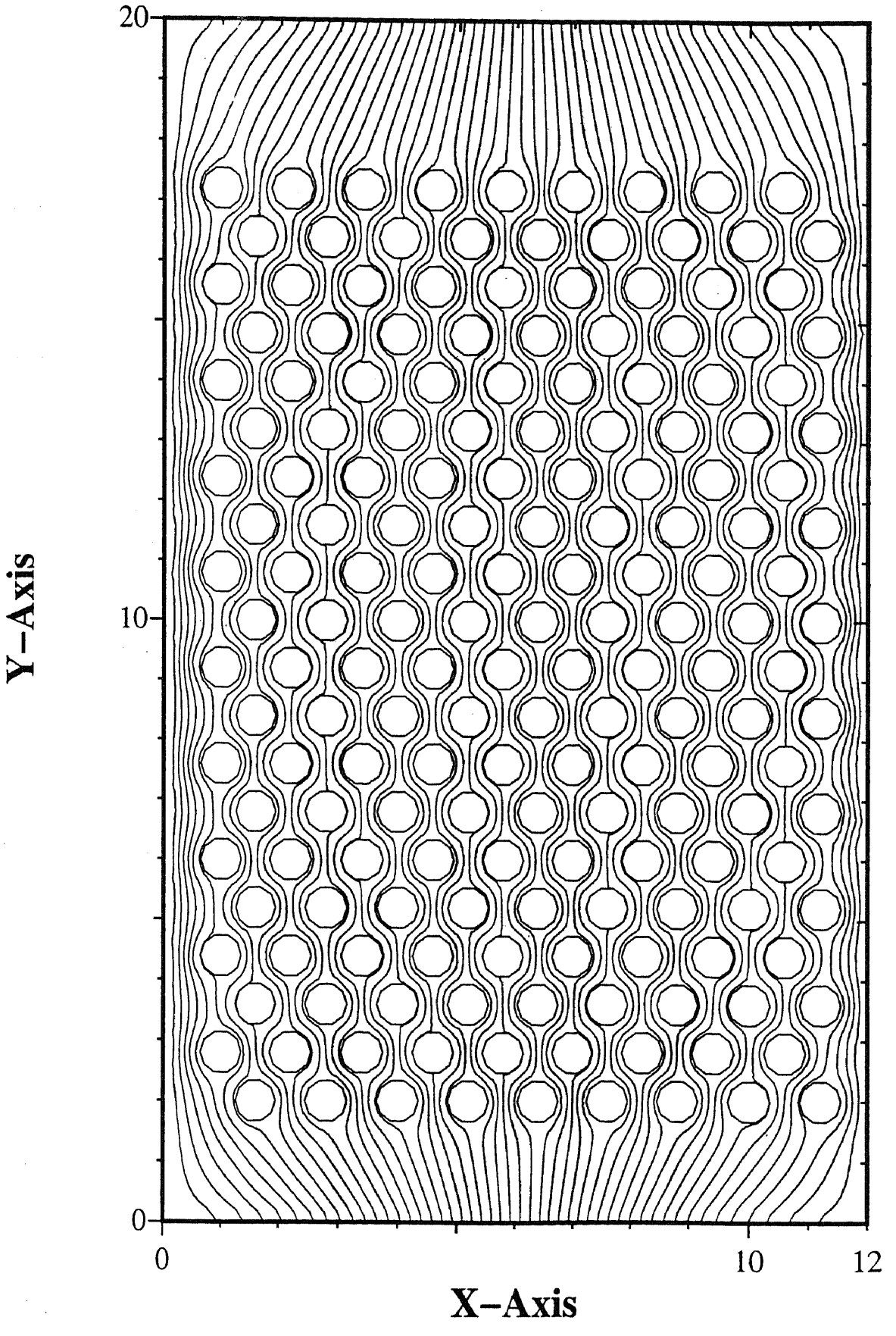

Figure A-3 Filter stream lines for Reynolds number=1

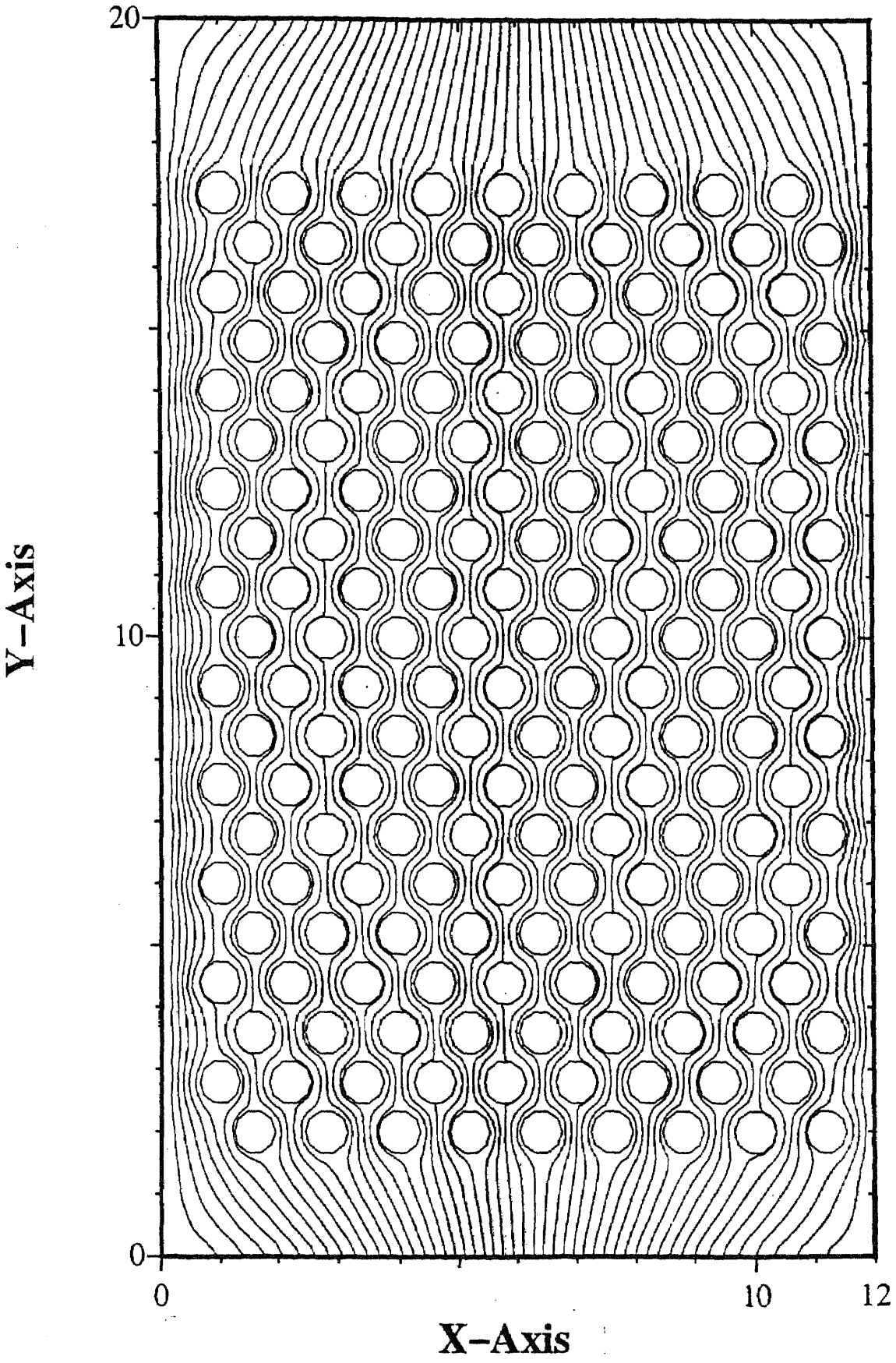

Figure A-4 Filter stream lines for Reynolds number=16.556

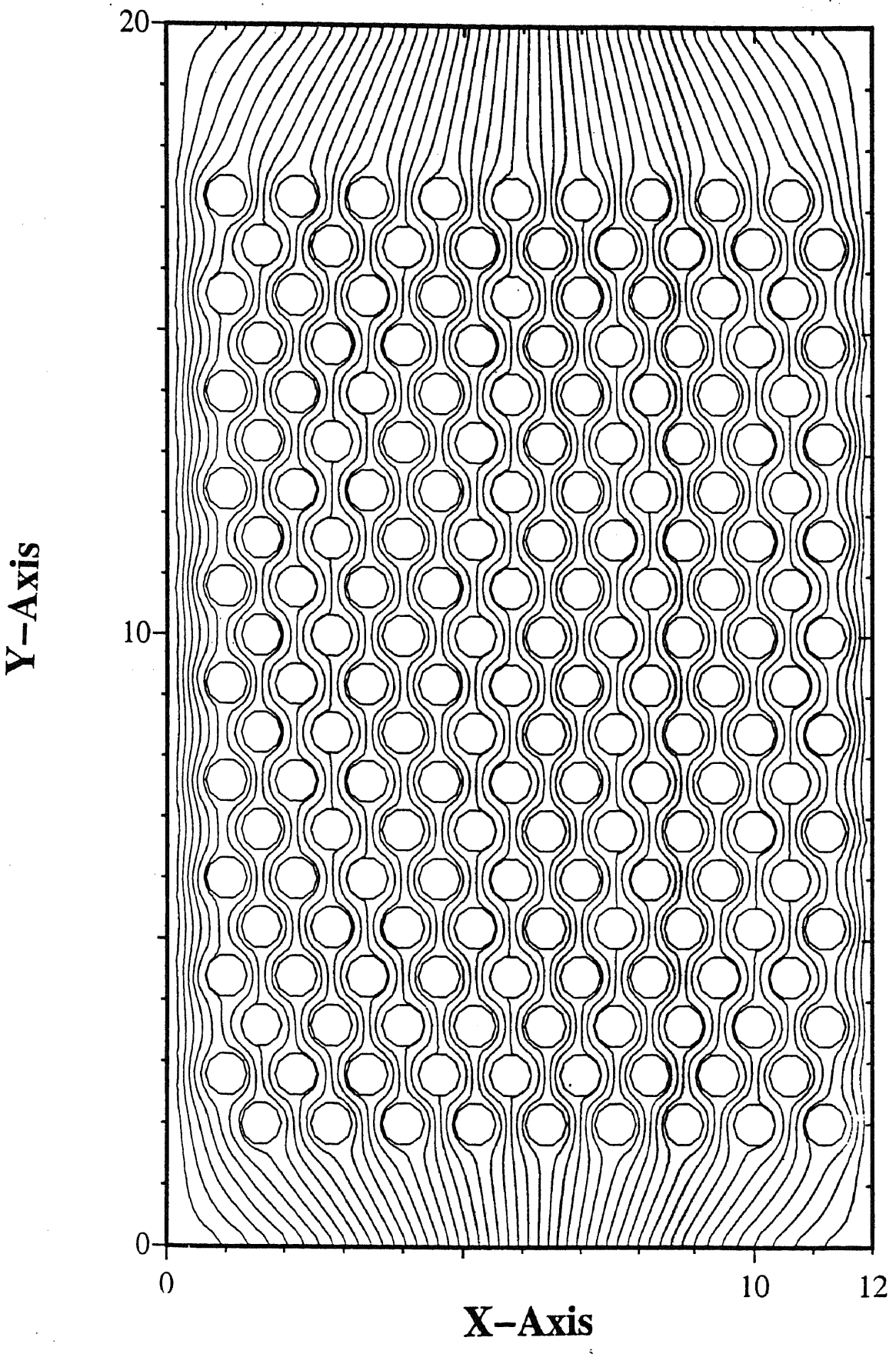

Figure A-5 Filter stream lines for Reynolds number=100

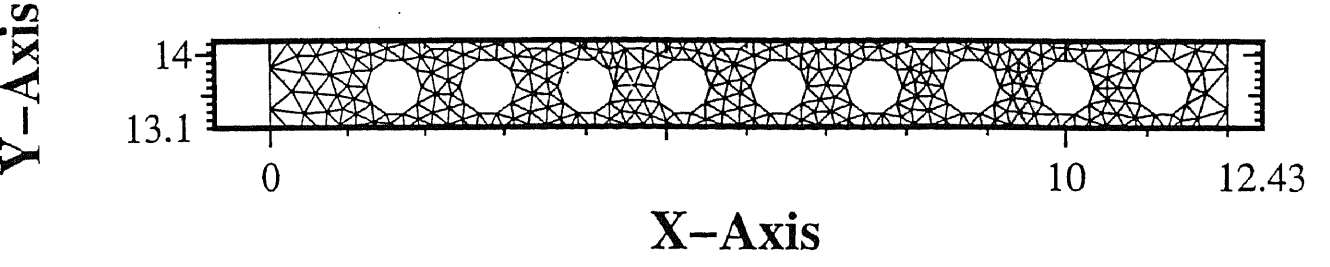

Figure A-6 One Unit Bed Element (No.4 UBE)

APPENDIX B

SIMULATION PARAMETER AND RESULTS FOR REYNOLDS NUMBER =1

Table 1 List of parameter (Reynolds number = 1)

Reynolds number	1
Drag coefficient	20
r	0.001~0.5
Flow direction	Down flow
Δt	0.001~0.1
Number or particles	500~100000
Efficiency	0.666667~1

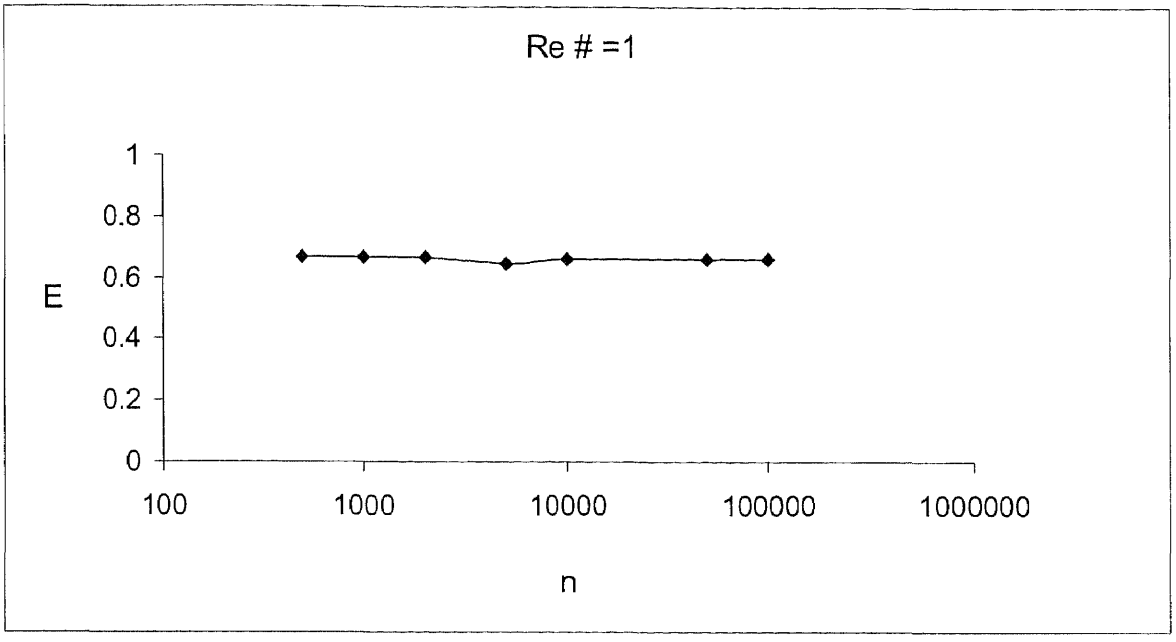

Figure B-1 Numerical results for number of particles injected. When we injected 500~100000. (C_D=20, Δt=0.001 and r=0.001)

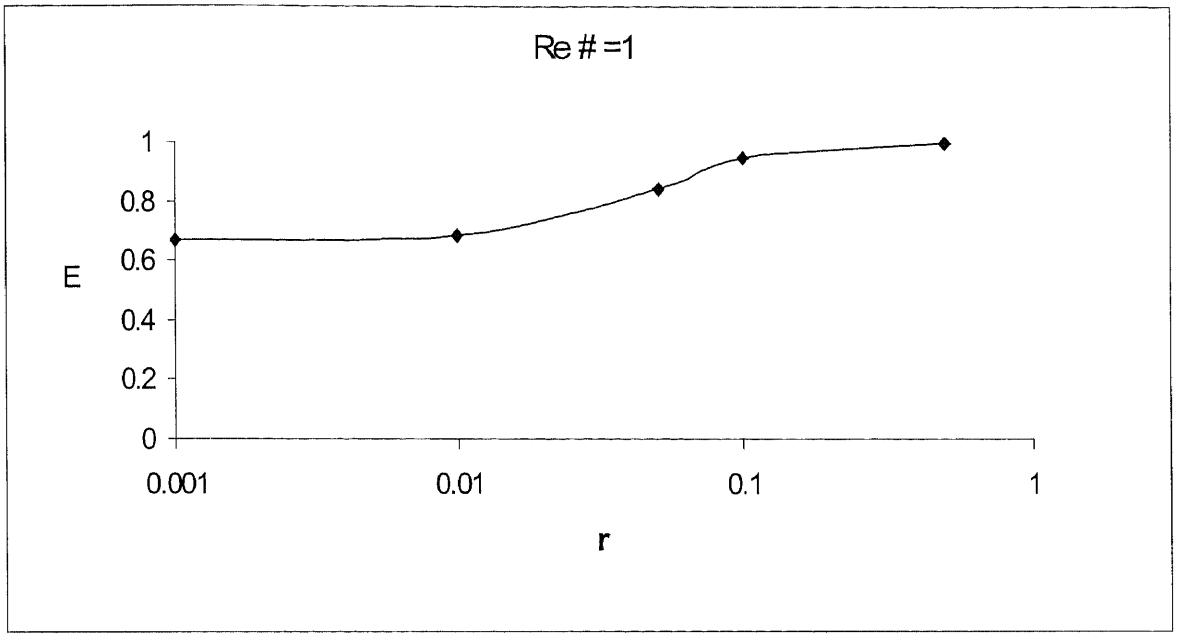

Figure B-2. Numerical results for the radius of particles injected. (n=500, C_D=20, Δt=0.001 and r=0.001~0.5)

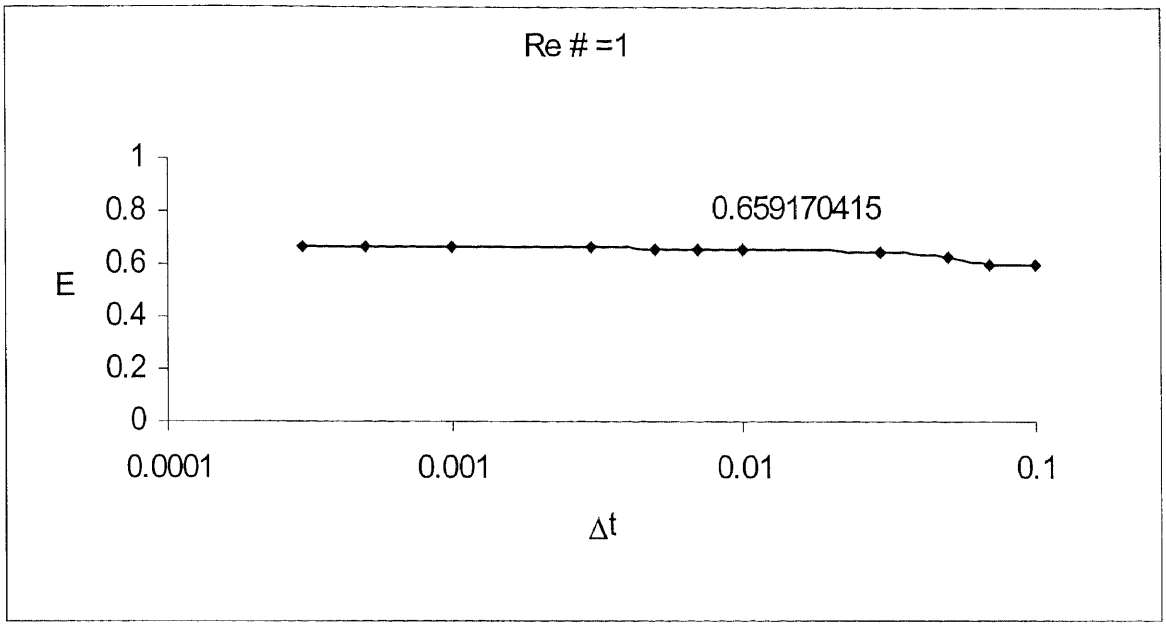

Figure B-3 Numerical results for the different Δt. (n=500,C_D=20, Δt=0.0001~0.1 and r=0.001)

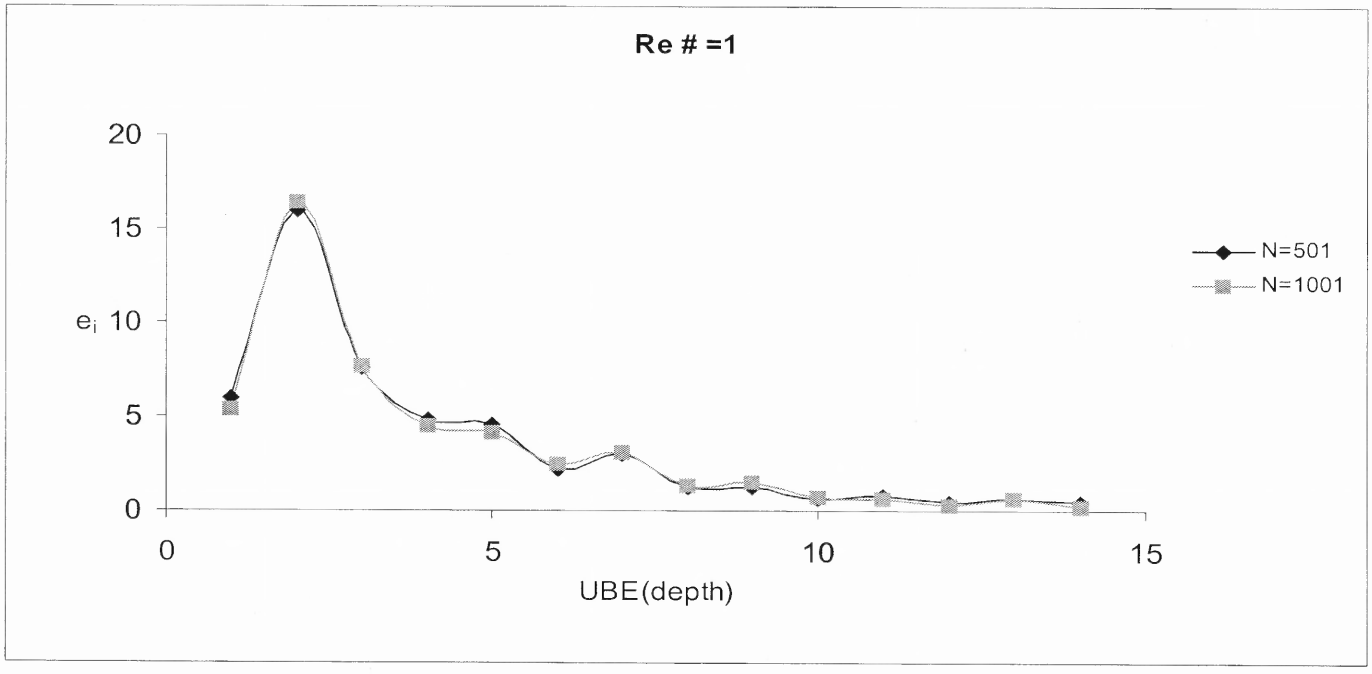

Figure B-4 Numerical results for the particle penetration depths for Reynolds number = 1

APPENDIX C

SIMULATION PARAMETER AND RESULTS FOR REYNOLDS NUMBER =16.556

Table 1 List of parameter (Reynolds number = 1)

Reynolds number	**16.556**
Drag coefficient	**20**
r	**0.001~0.5**
Flow direction	**Down flow**
Δt	**0.001~0.1**
Number or particles	**500~100000**
Efficiency	**0.550898~1**

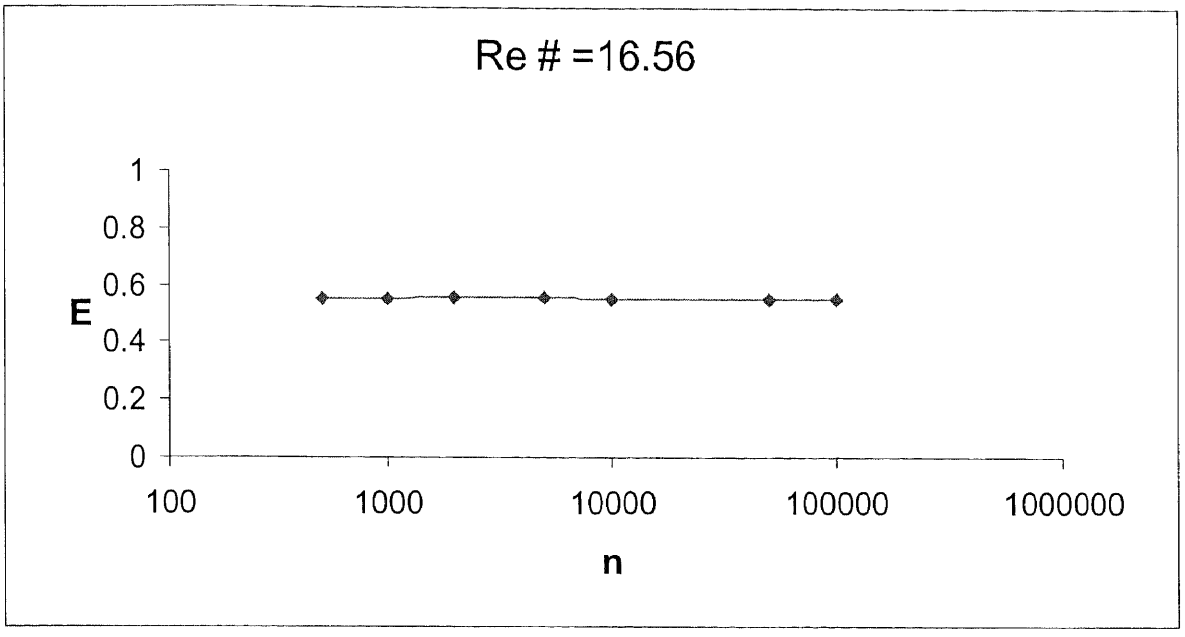

Figure C-1 Numerical results for number of particles injected. When we injected 500 ~100000. (C_D=20, Δt=0.001 and r=0.001)

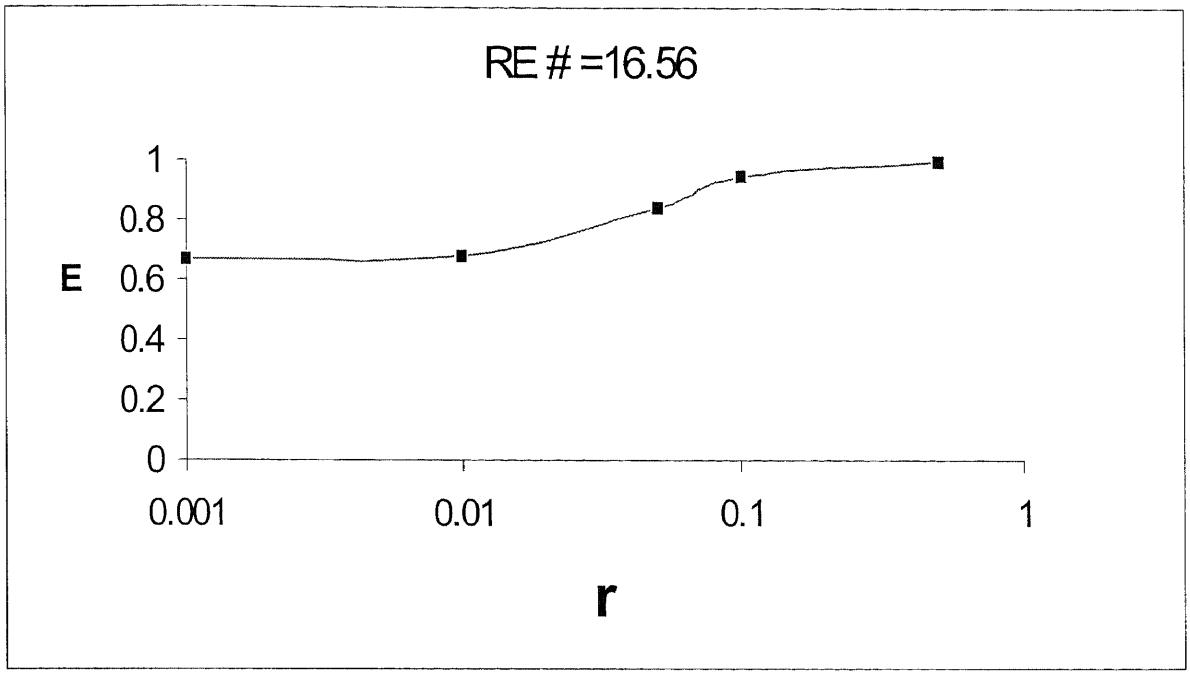

Figure C-2 Numerical results for the radius of particle injected. (n=500, C_D=20, Δt=0.001 and r=0.001~0.5)

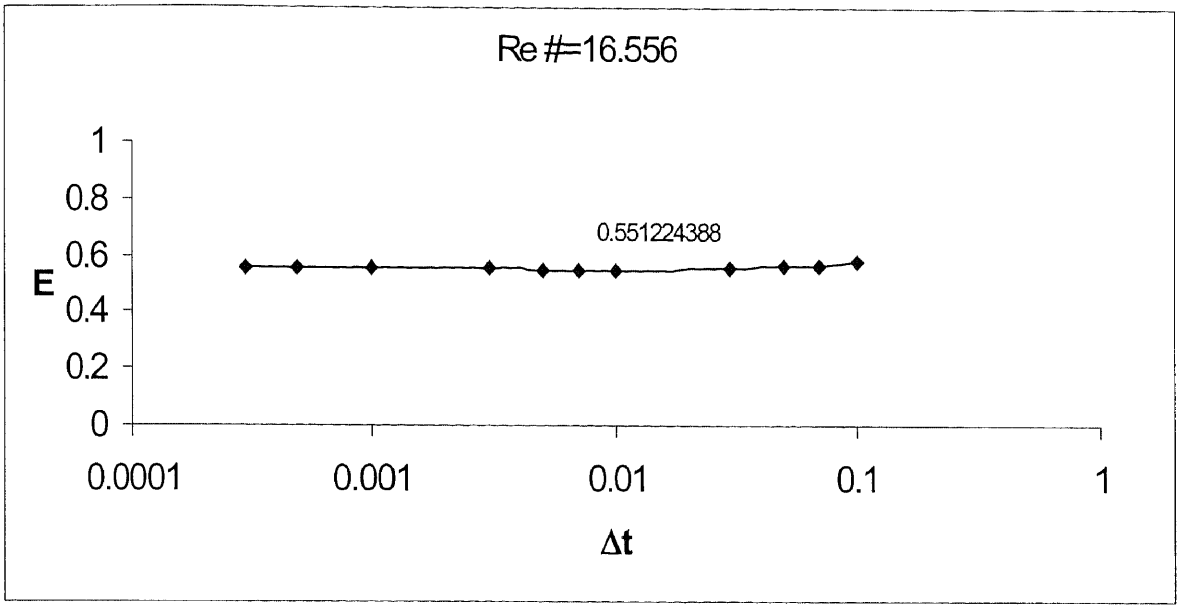

Figure C-3 Numerical results for the different Δt. (n=500,C_D=20, Δt=0.0001~0.1 and r=0.001)

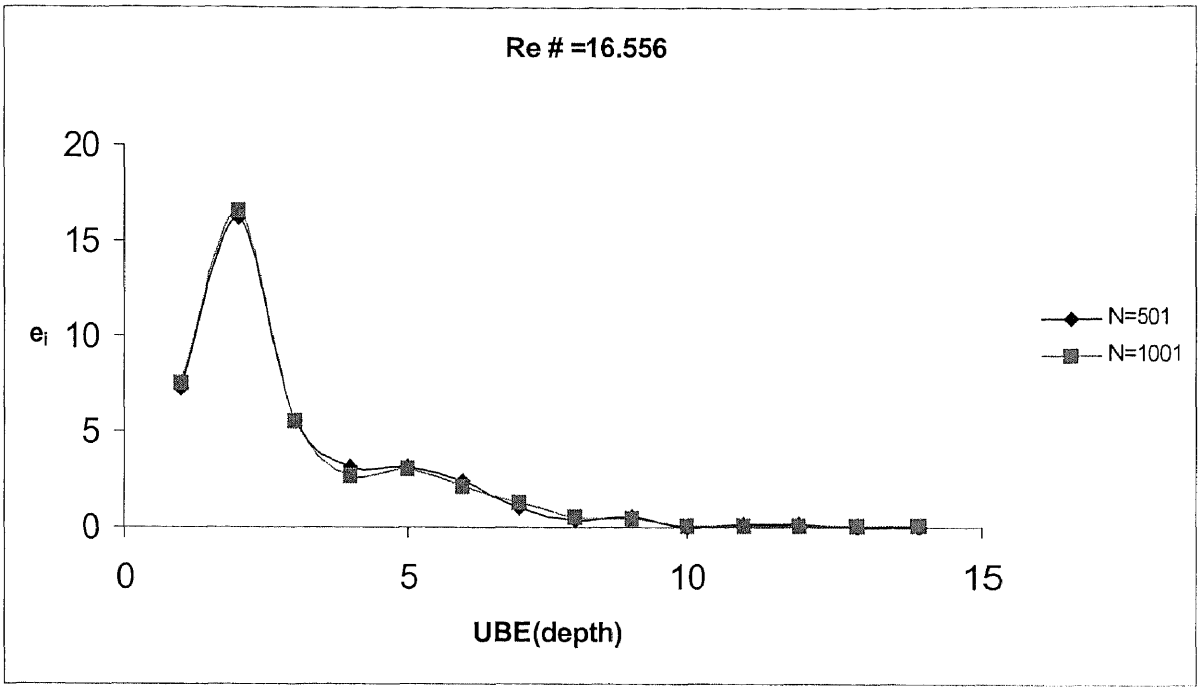

Figure C-4 Numerical results for the particle penetration depths for Reynolds number = 16.556

APPENDIX D

SIMULATION PARAMETER AND RESULTS FOR REYNOLDS NUMBER =100

Table 1 List of parameter (Reynolds number = 1)

Reynolds number	**100**
Drag coefficient	**20**
r	**0.001~0.5**
Flow direction	**Down flow**
Δt	**0.001~0.1**
Number or particles	**500~100000**
Efficiency	**0.540918~1**

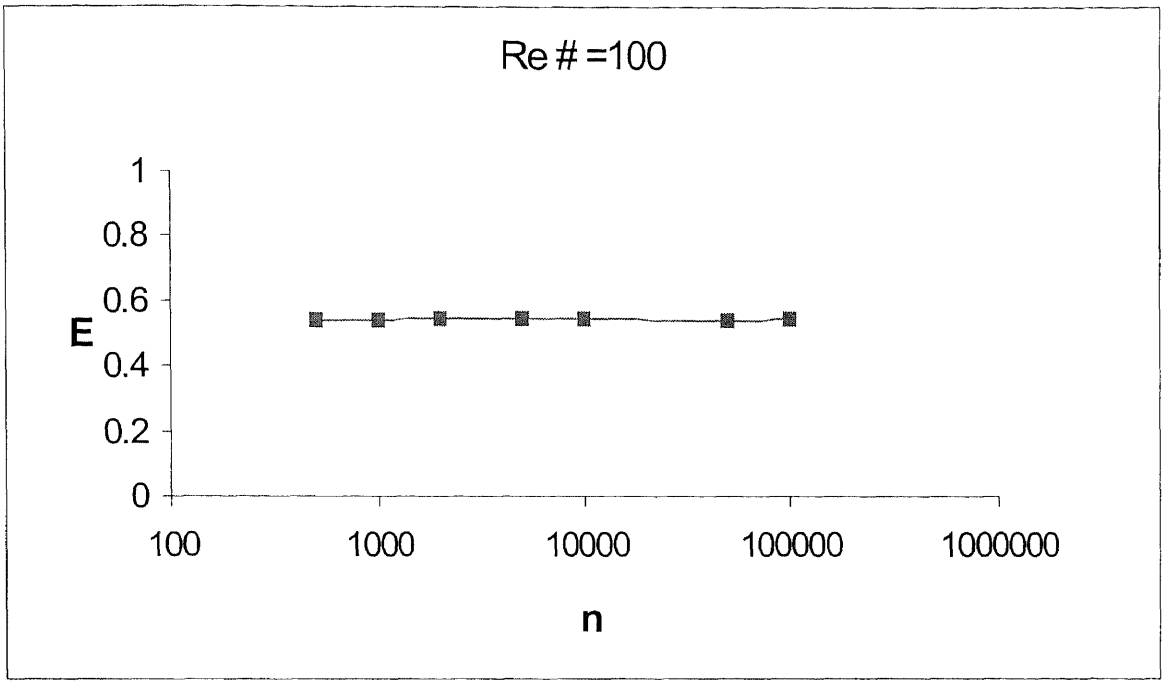

Figure D-1 Numerical results for number of particles injected. When we injected 500 ~100000. (C_D=20, Δt=0.001 and r=0.001)

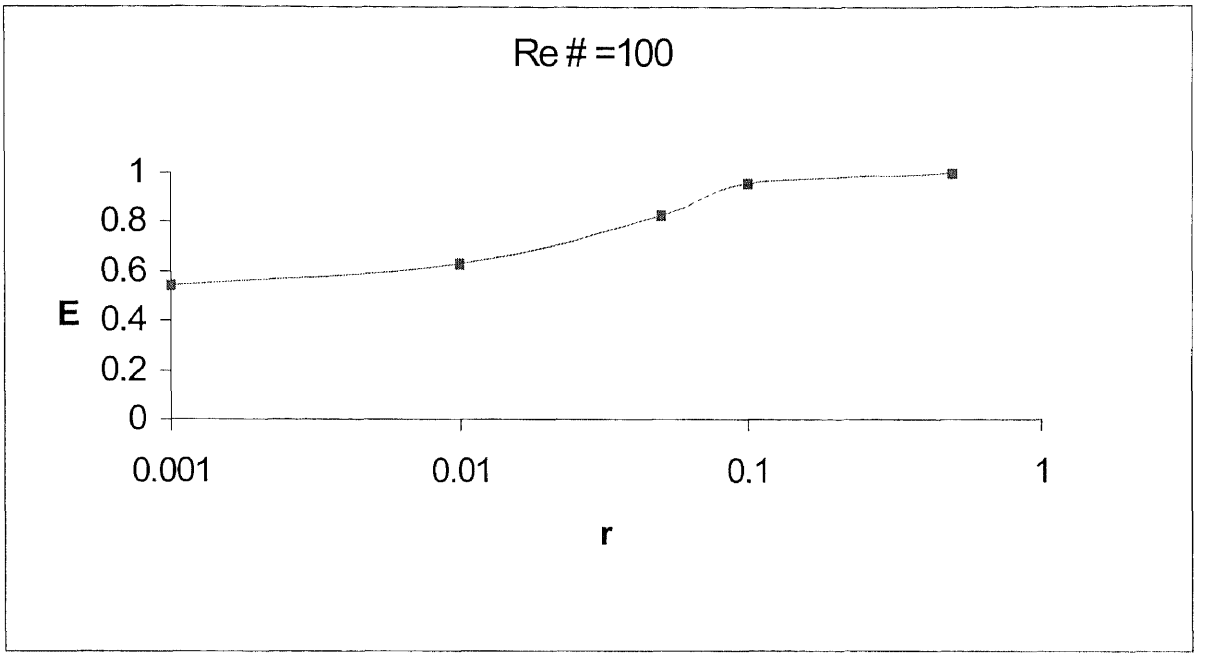

Figure D-2 Numerical results for the radius of particle injected. (n=500, C_D=20, Δt=0.001 and r=0.001~0.5)

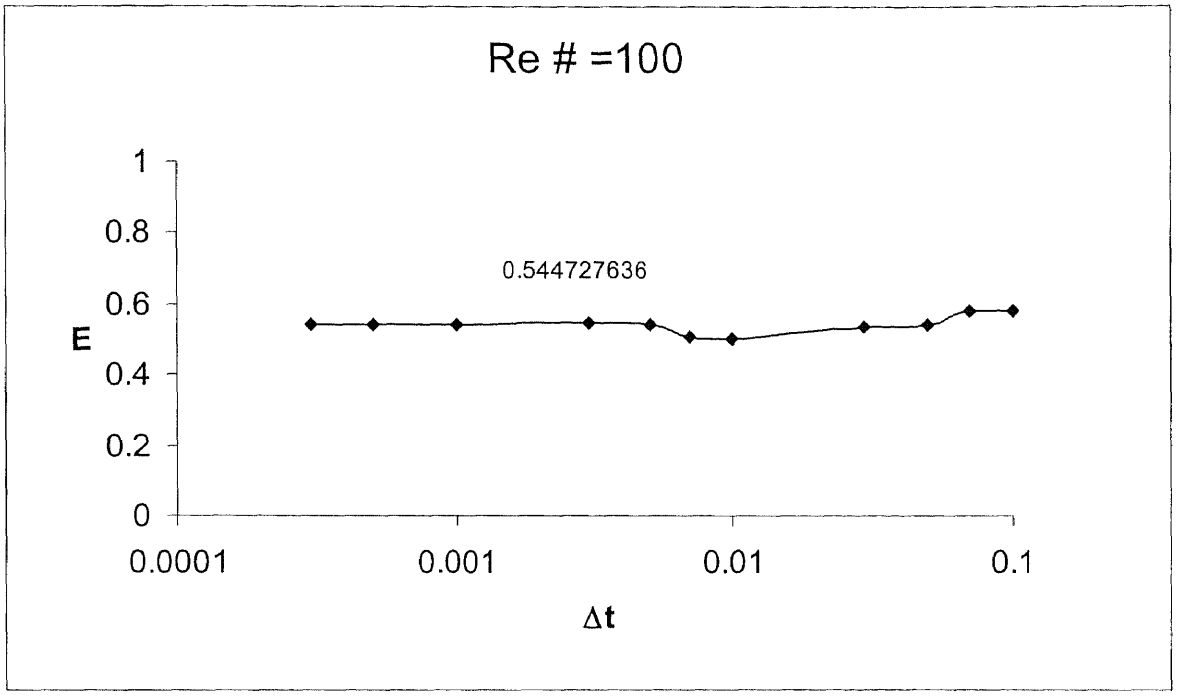

Figure D-3 Numerical results for the different Δt. (n=500,C_D=20, Δt=0.0001~0.1 and r=0.001)

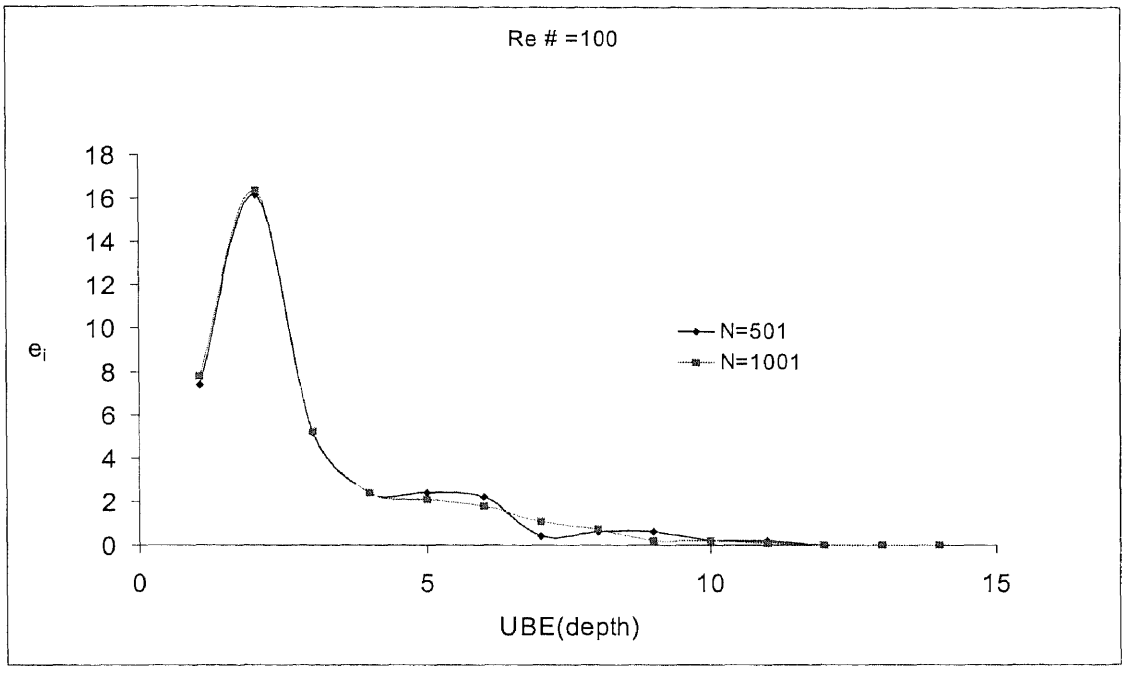

Figure D-4 Numerical results for the particle penetration depths for Reynolds number = 100.

REFERENCES

1. Claude Ghidaglia, Lucilla de Arcangelis, Johe Hinch, and Elisabeth Guazzelli "Hydrodynamic interactions in deep bed filteration" *Phys. Fluids*, vol. 8, No.1, pp. 6-14, 1996.

2. Rajamani rajagopalan and Chi Tien "Trajectory analysis of deep bed filtration with the shphere-in-cell porous media model" *AIChE Journal*, vol 22, No. 3, pp. 523-533, 1976.

3. A.O.Imdakm and Muhammad Sahimi "Transport of large particles in flow through porous media" *Physical Review A* , vol. 36, No. 11, pp.5304-5309, 1987.

4. E, Gal, G. Tardos and R. Pfeffer "A study of inertial effects in granular bed filtration" *AIChE Journal*, vol. 31, No. 7, pp. 1093-1104, 1985.

5. Hemant Pendse, Chi Tien and R. M. Turian "Drag force measurement of single spherical collectors with deposited particles" *AIChE Journal*, vol. 27, No.3, pp 364-372, 1981.

6. Chi Tien and Alkiviades C. Payatakes "Advances in deep bed filtration" *AIChE Journal*, vol. 25, No. 5, pp. 737-759, 1979.

7. J. P. Herzig, D. M. Leclerc and P. Le Goff "Flow of suspensions through porous media application to deep filtration" *Industrial and Engineering Chemistry*, vol. 62, No. 5, pp. 8-35, 1970.

8. C. S. P. Ojha and N. J. D. Graham "Computer-aided simulation of slow sand filter performance" *Wat. Res.* vol. 28, No. 5, pp. 1025-1030, 1994.

9. Hemant Pendse and Chi Tien "General correlation of the initial collection Efficiency of Granular filter bed." *AIChE Journal* vol.28 No. 4 pp. 677-686, 1982.

10. Yao, K.M., et al., " Water and wastewater filtration: concepts and application," *Environ. Sci. Technol.,* No. 5, pp.1105, 1971.

11. Bellamy W. D., Hendricks D. W. and Logsdon G.S. "Slow sand filtration : influences of selected process variables" *Journal Am. Wat. Wks Ass.* No. 77 pp.62-66, 1985.

12. Huisman L. and Wood W. E. *Slow sand filtration* World health organization, Geneva. 1974.

13. Hendricks D. W., Ed. *Manual of design for slow sand filtration* AWWA Research Foundation and American Water Works Association, U.S.A. 1991.

14. Logsdon G.S., Ed. *Slow sand filtration: Manual of practice* American Society of Civil Engineers, New York, U.S.A. 1991

15. Woodward C. A and Ta C. T. Developments in modeling slow sand filtration: *In Slow Sand Filtration Recent Developments in Water Treatment Technology* (Edited by Graham N. J. D.), pp. 349-366. Ellis Horwood, U.K. 1988.